QUILL

Quarterly Reports

February – April 2021

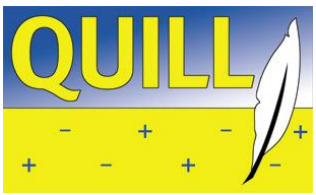

Contents

QUILL Quarterly Report

February 2021 – April 2021

Name:	Haris Amir		
Supervisor(s):	Prof John Holbrey		
Position:	Postgraduate (PhD)		
Start date:	01/10/2020	Anticipated end date:	30/09/2023
Funding body:	ESPRC/UKRI		

Synthesis of new boron containing anions

New boron containing anions are of interest for the development of new ionic liquid anions with a wide range of potential applications including electro- and photo- chemistry, separations and extraction of metals and waste. In this work, boron(III)-coordination with chelating oxygen/nitrogen donors in a four-coordinate environment has been investigated.

The formation of alkali salts of different borate anions incorporating O- and N/O- donor ligands is described. Then cation exchange of the alkali metal with tetrabutylphosphonium $[P_{4444}]^+$ cation is discussed, to promote crystallisation and carry out single crystal XRD studies.

Borate anions were synthesised initially in their acid form via esterification reaction involving boric acid and various ligands. The ones that have been successfully synthesised are shown in figure 1.

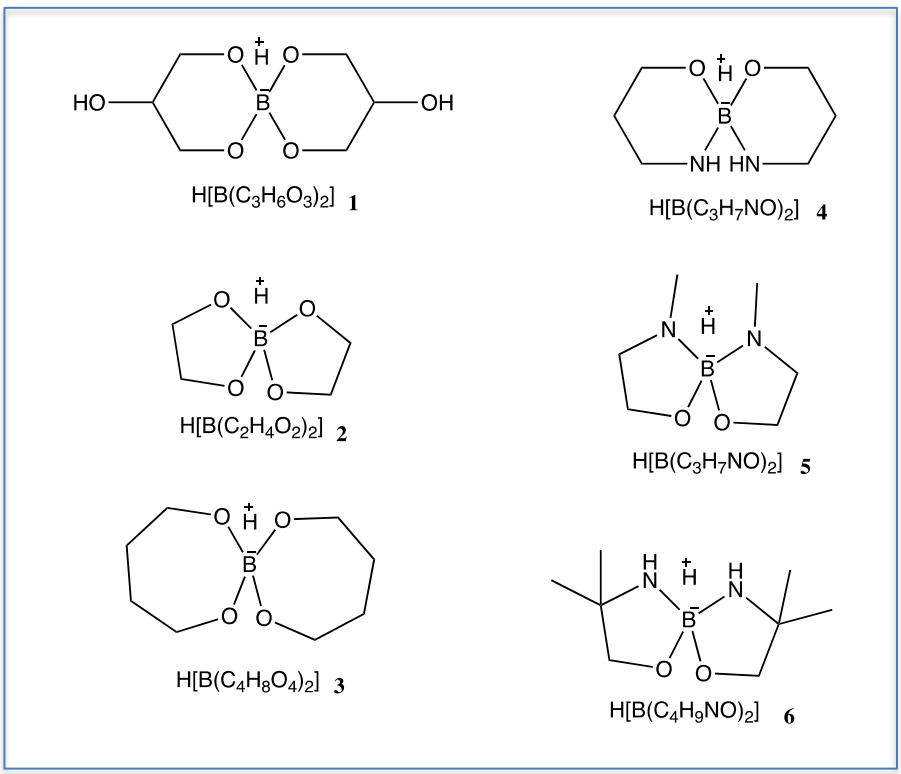

Figure 1 - The structure of borate ester anions

On the surface these reactions looked to be successful. However, upon further reading it was found that 4-coordinate boron anions typically have signals in the region of δ 0-10 ppm. While 3-coordinate boron compounds have signals within the region of δ 13-20 ppm. Based on an interpretation of results reported by Ishii *et al.*, Wu *et al.* and Miyazaki *et al.*,[1-3] instead of the proposed 4-coordinate borate anion. The 3-coordinate boron compounds are obtained. It is known that borate esters are readily hydrolysed with even trace amounts of water, and from this it can be hypothesised that when the 4-coordinate borate anions are formed, the free proton breaks the B-O/N bond leading to the formation of the neutral 3-coordinate borate compound. This is likely to be in equilibrium, where the equilibrium shift is dependent on the concentration of the free H^+ ions. Figure 2 shows two proposed equilibria between the 4- and 3- coordinate boron species. The first is in the presence of water and the second is without.

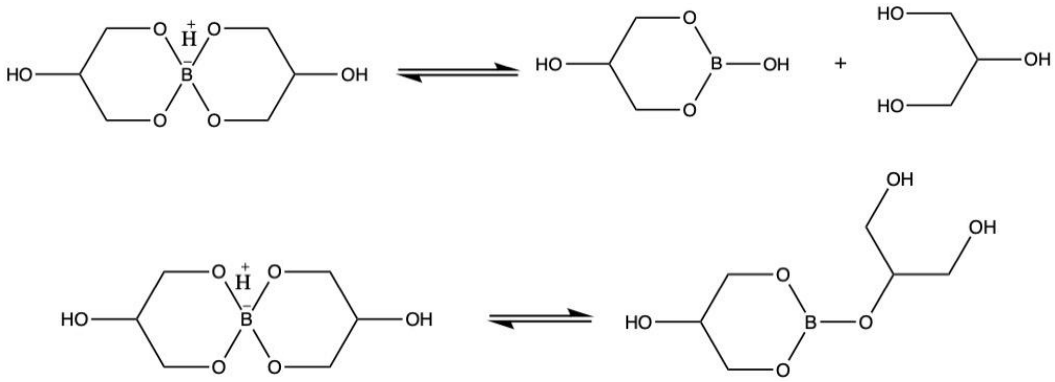

Figure 2 -The dissociation of a 4-coordinate borate anion in the presence of water and without.

This issue was overcome by the formation of salt versions of the borate anion, each anion in figure 1 was reacted with KOH to produce an alkali salt of the anion. The ^{11}B NMR before and after reacting KOH for each derivative is shown in table 1.

Table 1 - The δ ^{11}B NMR of borate esters before and after reacting with KOH

Borate ester	δ ^{11}B NMR (ppm)	Alkali salt of borate ester	δ ^{11}B NMR (ppm)
$[H][B(gly)_2]$	19.38	$K[B(gly)_2]$	5.23
$[H][B(C_4H_8O_2)_2]$	18.14	$K[B(C_4H_8O_2)_2]$	4.54
$[H][B(C_2H_4O_2)_2]$	18.56	$K[B(C_2H_4O_2)_2]$	4.78
$[H][B(C_2H_9NO)_2]$	14.56	$K[B(C_2H_9NO)_2]$	3.03
$[H][B(C_3H_7NO)_2]$	19.56	$K[B(C_3H_7NO)_2]$	4.95
$[H][B(C_3H_7NO)_2]$	19.42	$K[B(C_3H_7NO)_2]$	3.97

Table 1 validates the proposed hypothesis, the table shows the NMR results with a series of O- and N/O- binding ligands to the boron. In each case the acid form shows characteristics of the presumably neutral three-coordinate boron species (chemical shifts in the region 15-20 ppm) whereas forming the alkaline metal salt in systems where the boron centre reports ^{11}B δ between

3-5.5 ppm. This is consistent with formation of four-coordinate boron which can be directly interpreted as anion formation.

Each of these borate anions were mixed with tetrabutylphosphonium chloride $[P_{4444}]Cl$ to exchange the alkali metal with a phosphonium cation. This cation is not ideal to form ionic liquids but rather to produce crystals of the molten salts. Once the crystals were isolated by drying on a Schlenk line single crystal XRD was performed to obtain structural characteristics of the borate anion. Single crystal X-ray analysis is currently underway.

Future work

Future work will be to carry out further investigations to test the hypothesis. Along with obtaining the crystal structure of the remaining borate anions. In addition, thermogravimetric analysis (TGA) and Differential scanning calorimetry (DSC) analysis will be run on the ionic liquids. Lastly a range of diamines will be used as ligands to form borate anions with just N-donors to complement the O and O/N-donor sets.

References

1. T. Ishii and H. Ono, *Carbohydrate Research*, 1999, **321**, 257–260.
2. W. Xu, L.-M. Wang, R. A. Nieman and C. A. Angell, *The Journal of Physical Chemistry B*, 2003, **107**, 11749–11756.
3. Y. Miyazaki, K. Yoshimura, Y. Miura, H. Sakashita and K. Ishimaru, *Polyhedron*, 2003, **22**, 909–916.

QUILL Quarterly Report

February 2021 – April 2021

Name:	Marian Borucki		
Supervisor(s):	Prof Peter Nockemann, Dr Stephen Glover & Dr Małgorzata Swadźba-Kwaśny		
Position:	PGR Student		
Start date:	01.2018	Anticipated end date:	09.2021
Funding body:	Bryden Centre, Horiba Mira		

Lithium ion batteries degradation study using spectroscopy techniques

Background

Lithium ion batteries (LIB) are a secondary (rechargeable) battery that are currently the main energy storage device. LIBs are applied in various applications as in portable devices, grid energy storage, grid current regulation as well as in hybrid- and electric vehicles. Energy harvested by the renewable energies is often environmental dependent, what results in discontinuous energy supply. In order to store energy that have been over generated during less energy consuming times of a day, energy storage stations based on LIB are used. The other, yet not less important, application is one where LIBs are replacing the fossil fuel by storing the energy for transport sector, namely in hybrid (HEV) and electric vehicles (EV). The trend of replacing the fossil fuels both in energy sector by supplementing them with renewable energy power plants as well as by supporting the market of HEV, EV and fuel-cell vehicles (FCEV) is growing. New policies of EV30@30 and New Policy Scenario are the programmes that are aimed in expanding the market of HEV, EV and FCEV, thus the supply for lithium ion batteries will grow. Yet, for the market to growth the research, ones that solve current issues, are needed. Automotive council UK in their roadmap report for the lithium ion batteries have gathered up the issues that are needed to be addressed if the automotive of EV, HEV and FCEV is to grow. Such an issues are based on the need of improving the safety of battery usage, lowering the costs of the batteries, researching a new materials for the batteries that will allow to store more energy and provide more power, thus be fast chargeable, issues concerning the battery pack and modules combination, one that will allow to minimalize the losses related to cell joining, as well as their thermal management, increasing the lifespan of the batteries as well as increase their recyclability, eventually the research on the next gen batteries is needed.

In order to meet all the requirements a thrill study of the current batteries as well as the development of a new chemistries is needed. Lifespan as well as the safety of the battery is nowadays ones of the most important factor when it comes to the battery application in the transportation market. Battery life is limited by the degradation mechanism, ones that occur inside the cell. Currently there are known number of such mechanism occurring, even though the proper investigating technique allowing *in operando* study have not been developed yet. Moreover, the degradation is highly chemistry dependent so whenever the new chemistry is tested for the battery the new degradation mechanism could occur. On the other hand, the safety of the battery is limited by the usage of the organic based electrolyte, which is highly flammable and might lead to battery explosion. Proper electrolyte, non-toxic, environmentally friendly, non-flammable as well as of high performance should be developed. With developing the new electrolyte, often the development of

the electrodes is needed as the electrolyte stability as well as the energy density of the battery highly depends on them.

Objective of this work

The aim of the PhD programme is focused on investigating the lithium ion battery (LIB) degradation processes occurring inside the cell during it operation. In order to achieve the goal a development of an experimental method basing on the spectroscopy analysis techniques will be needed. A proper method would allow to observe and measure the changes that occur *in operando* inside the lithium ion battery. During the PhD programme an analytical data of LIB degradation will be acquired, using various analytical techniques including electrode surface examination, electrolyte composition. Acquired spectroscopy data will be linked with the rest of the data gathered in order to develop the sensing method. Eventually, batteries of a different cell chemistries will be investigated.

Back to laboratory work

Electrochemical studies – Following the impact of SoC level on impedance spectra investigation, the temperature dependency of an impedance has been studied for half and full cells within 25℃ - 55℃ temperature range.

***Post-mortem* studies** – The *post-mortem* case has been designed, 3D printed and tested for laser beam permittivity using Witech alpha 300R microscope with a control sample as for leakage proving to be sealed. The aged samples are planned to be dismantled in a glovebox. The electrodes are to be sliced in half using ceramic knife into two parts. A four samples, two for cathode and two for anode, are expected to be obtained per sample. The as prepared post-mortem samples are to be used for spectroscopy data collection as well as for structural microscopy studies and crystallographic studies. The obtained data from *post-mortem* studies would provide insights to the specific degradation processes occurring inside the cell as the cell is aged and could be further compared to electrochemical data obtain during sample ageing. Due to high sensitivity of XPS study, which is aimed to investigate the top layer (10nm) of electrodes providing insights into interfacial film properties as the electrodes are aged, the dismantling of aged cells has been postponed until access to XPS will be gained.

Semi-solid electrolyte 'Ionogel' studies – Mechanical properties investigation in cooperation with school of aerospace and mechanical engineering in planning as interschool laboratory access is limited. Synthesis optimization – establishing the substrates molar ratio which result in product of highest ionic conductivity as well as the most optimal mechanical characteristics. Lithium transference number for electrolytes of each substrate ratio is needed to be studied.

Carbon-based anodes electrochemical investigation – The coating of carbonaceous material on copper foil is investigated for electrode preparation.

***In operando* studies – Cell Design** – The reshaping of an optical window material was investigated at first. The thickness of acquired quartz glass is $150\ \mu m$, therefore cutting by the use of the standard glass cutting tools become impossible. Additionally, of being very thin layer material do display high brittleness. The reshaping a material, by cutting its sharp edges eventually forming a disc of a 16 mm diameter has been investigated using laser cuter. The laser cut of the quarts, however it's not a trivial task due to low absorption levels for the material. However, it was believed that with experimentation an optimal laser power can be found. Unfortunately, due to high laser power needed the glass melted, whereas lower laser power was not able to cut through the

material. Eventually the investigation has proven for laser cut to not be a suitable approach for reshaping quartz glass to the desired shape. After consideration of the options, it has been decided to not reshape the glass, yet to reshape the cell design for the glass to fit the cell.

The electrode shapes have been designed as seen at. The cutting of the electrodes to the desired shape was meant to be done using a specially made die to the press. Unfortunately, the price of die manufacture has resulted in search for alternatives. The laser cutter was again used in order to cut the electrodes to the shape. The electrode martial have been sandwiched between two sheets of aluminium of 2 mm thickness which would serve a protective layer and heat acceptor material. Unfortunately, the cutting of the electrodes by laser cutter, although successful have damaged the electrodes in the extend that would impact its performance. Final alternative for the electrode cutting is in designing a stamp that would allow as a template and further use of the foil cutting tools. The stamp has been designed and 3D printed. The metal foil ceramic knife cutter has been used to cut the shape out of stamp, Figure 1B.

The sample parts as internal and external casing and gasket has been designed and 3D printed. For the assembly purposes six M6 stainless steel bolts with washers has been used. The assembly has been carried out in the argon atmosphere of glovebox. The first design could be seen on Figure 2C. However, due to fragile nature of copper and aluminium current collectors, the cell needed to be upgraded.

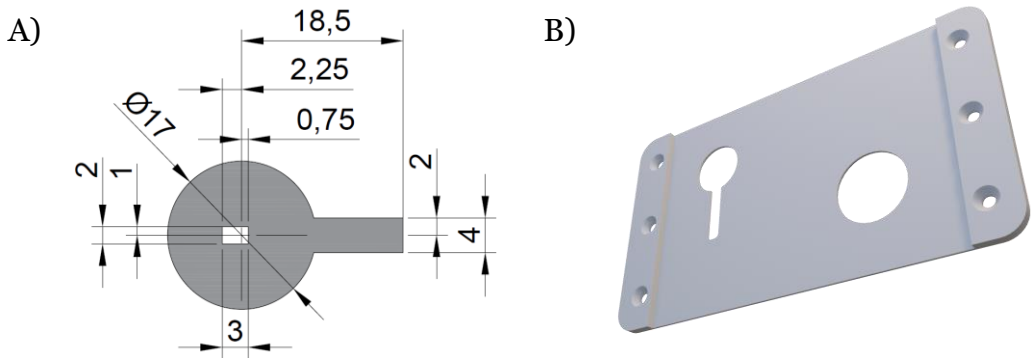

Figure 1 - In operando coin cell design: A) Schematic of the electrode shape, B) STL of an electrode cutting stamp.

The first approach was to solder an extension wires to the external outputs, so the sample would not be directly connected to battery tester. Soldering a thin foil of aluminium in the glovebox environment has been found to be impossible s the aluminium melt and broke easily. The following approach to the cell design was to add a stainless steel support. The support piece has been designed and further water jet cut by workshop at School of Mechanical & Aerospace Engineering. The internal casing design has been updated to fill in the stainless steel support. The updated design could be seen on Figure 2A and the assembled sample on Figure 2D the samples has been assembled, yet the performance instability of cells has been observed. The instability is believed to be from low contact area between support, which also act as a current collector with copper/aluminium. To counteract the low contact area a new design for both internal cell casing and a stainless steel support has been implemented as it could be seen on Figure 2B. The cells of updated design are about to be put into the performance test.

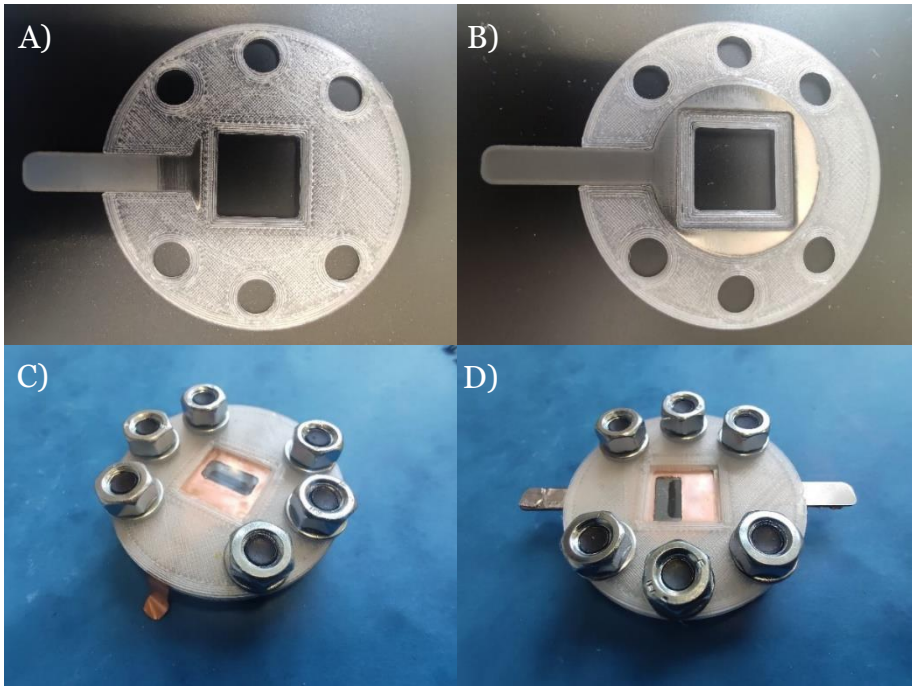

Figure 2 - The design of in operando spectroscopy lithium ion cell: A) the first internal design, B) an improved internal design, C) the first design of a cell, D) the latest cell design.

Eventually, the in operando cell design would allow for carrying on the experiment focused on studying the cell components by the use of spectroscopic techniques. The schematic of planned experiment, and illustration of cell mechanism of action could be observed on Figure 3. As it could be observed the designed battery has the same parameters as the coin cell battery (amount of electrolyte, electrodes area), although it possesses an asymmetric window on both sides with quartz glass that allows to obtain the background, cathode and anode spectrum while the battery is connected to the external circuit, thus to the battery tester and potentiostat measuring the battery properties and performing basic procedures of charging and discharging of the battery.

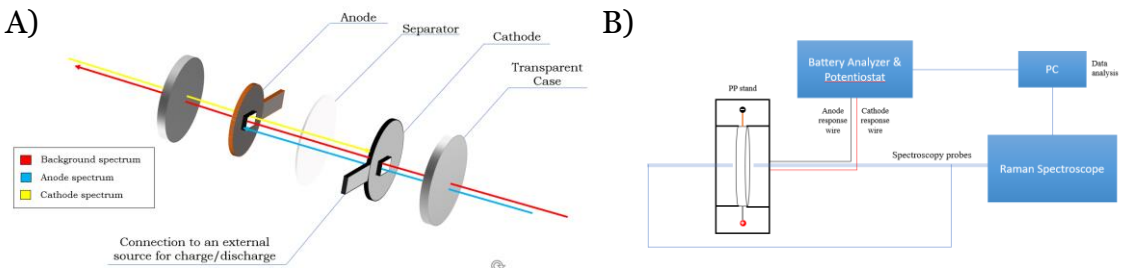

Figure 3 - Schematic of A) the transparent cell mechanism of action, B) experiment of LIB in operando spectroscopic studies

QUILL Quarterly Report

February 2021 – April 2021

Name:	Dominic Burns		
Supervisor(s):	Prof John Holbrey, Dr Gosia Swadźba-Kwaśny & Dr Hye Kyung Timken		
Position:	PhD Student		
Start date:	1st October 2019	Anticipated end date:	31st May 2023
Funding body:	EPSRC		

Recycle and Reuse of Process Water Through Sulfate Removal: Developing an Ionic Liquid Technology for Selective Anion Recognition and Extraction

This is an ESPRC industrial CASE project in collaboration with Chevron EL, to explore liquid technologies to treat saline process water with the initial objective of selective sulfate removal from highly competitive aqueous streams. Initial work began by characterising $[P_{66614}]Cl$ as a liquid anion exchanger. This work showed that sulfate can be extracted by $[P_{66614}]Cl$ from `ideal' sodium sulfate solutions via anion exchange as shown in the graph below. However, when chloride is already present in the aqueous phase this blocks the exchange process reducing the extraction to almost zero. To enhance these current approaches involve adding sulfate specific receptors into the IL phase to bind to the sulfate, micelle forming receptors that have previously been reported on and thiouronium ILs that are known to be good moieties for anion complexion.

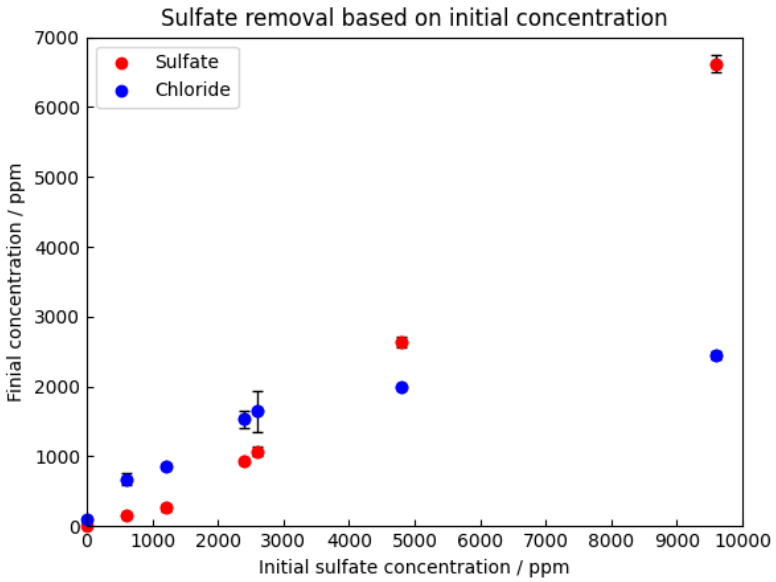

Previous work by Moyer *et al* (DOI: 10.1039/c8cc05115a) showed that a monofunctional di(imino)guanidinium micelle forming extractant can remove sulfate from aqueous solutions in the presence of chloride. This original extractant as well as 2 unalkylated analogues and 4 long chain analogues (shown below) have been synthesised. The purification of these final products is more difficult than expected as the benzaldehyde precursor have very similar properties to the final product and so column chromatography is not an effective separation technique for the required

amount of material. This approach has been put on hold until Isopar L solvent can be acquired and other approaches have been completed.

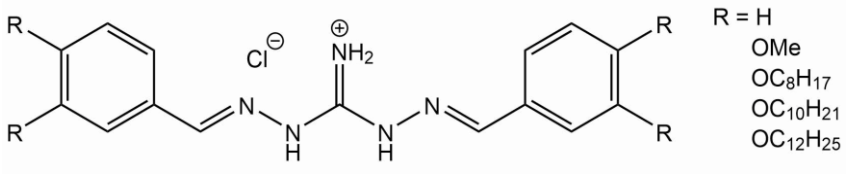

Thiouronium ILs and carboxylate receptors have previously been reported by QUILL researchers (DOIs: 10.1039/c0nj00098a, 10.1039/c2nj40632b). Such moieties are known to be complementary to oxyanions with strong association constants. Previously made ILs (shown below) have been screened and found that shorter chain ILs where R^1 = ethyl/butyl and R^2 = methyl was too hydrophilic to be used as an extractant phase. Where R^1 = octyl and R^2 = ethyl this IL showed promise with leaching around 400 ppm but no apparent sulfate extraction. Increasing R^1 further only promoted the formation of emulsion phases making the analysis more difficult. Further research is now being carried out by a summer student to investigate ILs where R^2 = phenyl which increases the acidity of the NH groups leading to stronger binding.

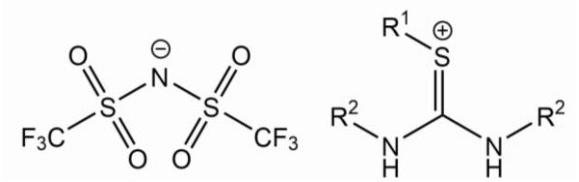

I have also worked with Dr Gosia Swadźba-Kwaśny, Miss Shannon McLaughlin and Mr Haris Amir with the Institute for Research in Schools (IRIS) on a protic ionic liquid project (https://researchinschools.org/projects/ionic-liquids/) to enhance interest and participation of secondary school children in chemistry. The project is based on previous QUILL work (DOI: 10.1039/c4gc00415a) where students will make protic ionic liquids by combining H_2SO_4 and amines and then use these as acid catalysts to form fragrant esters.

QUILL Quarterly Report

February 2021 – April 2021

Name:	Andrew Forde		
Supervisor(s):	Dr Stephen Glover, Dr Rob Watson & Prof Peter Nockemann		
Position:	PhD Student		
Start date:	03/06/2019	Anticipated end date:	03/12/22
Funding body:	Horiba-MIRA & EPSRC		

Battery Thermal Management and Algorithmic 3D Temperature Prediction

Experimental

One aim of this project is to place thermal sensors close to the active materials in a prismatic cell for model validation purposes. In order to carry this out, an instrumentation process has been designed and tested on a 3D printed model of the cell.

The chosen cell for this instrumentation work has changed, therefore the new cell was modelled for 3D printing. This will allow for testing of the instrumentation process on the new cell to ensure that the required accuracy can still be achieved. Safety checks have also been designed to ensure that the cell is fully sealed after being opened. Currently, gas chromatography is being investigated as a method for testing if battery internal gases are present after sealing the cell.

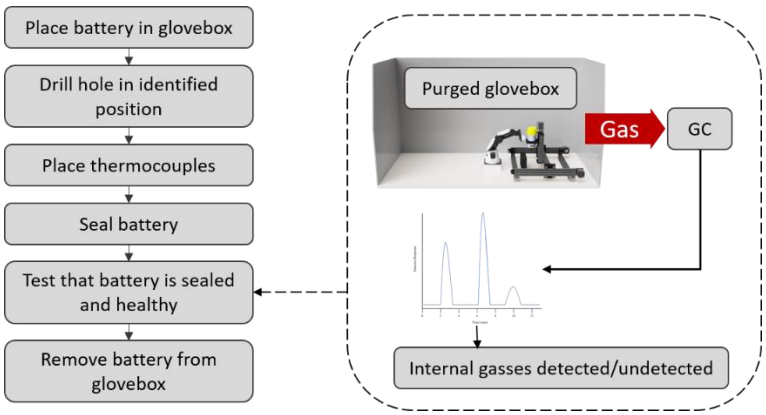

Figure 1 *- Gas chromatography method for testing battery seal*

In order to safely transport and store these cells, safety precautions must be met. After consulting with other academics experienced in battery experimental work, fire-safe battery storage bags were identified as a solution for storing a small number of cells. Lab space for carrying out this work was also identified along with required safety equipment to be used

Numerical Model

The numerical model used to simulate battery response has been updated to work with the new cell choice and modified to allow for easier changing between different cell chemistries and designs.

QUILL Quarterly Report

February 2021 – April 2021

Name:	Oisin Hamill		
Supervisor(s):	Dr Nancy Artioli & Dr Alex Goguet		
Position:	PhD		
Start date:	01/10/2019	Anticipated end date:	30/09/2022
Funding body:	EPSRC		

Mechanism Understanding of NOx storage, release and reduction on Pt/doped ceria catalysts

Due to strengthening emission legislations in Europe, North America and the rest of the world, there is a need for further optimisation of existing emission after-treatment catalytic converters for automotive applications. New legislations focus primarily of NO_X abatement and consequently the exhaust emissions of lean-burn gasoline and diesel vehicles. After treatments systems must utilise new technologies to reduce this that offer low temperature activation and high stability.

High surface area ceria is successfully employed as an excellent support of metals (Pd, Rh, Pt, etc.) in commercial catalytic systems for the oxidations of carbon monoxide and propane and automotive emission control. Ceria is a unique material with a rich and complex chemistry. It possesses high oxygen storage capacity (OSC), a unique redox property by the cycle of Ce^{4+}/Ce^{3+} redox pairs and it can be further enhanced through using dopants. Platinum supported on ceria can show enhanced NO_X storage at low temperature, as reported in the literature, together with an improved carbon monoxide/hydrocarbon light off.

Ceria supported catalysts, in general, do not operate efficiently at low temperatures and therefore must be modified in order to overcome this problem. For this reason, addition of enhancing materials is currently being considered in detail. This addition of a material that increases the performance of an already functional catalyst is called doping. The main function of this dopant is to allow the catalyst to function outside of the normal working temperature range and operating conditions to increase catalyst efficiency.

It has been proposed that the dopants, such as rare-earth and transition metal oxides, increase the concentration of surface vacancies which affect the ionic conductivity, oxygen mobility and oxygen storage capacity of the ceria. It can be speculated that all these properties are responsible for the enhanced oxidation activity by promoting oxygen diffusion and formation of more "reactive oxygen" species. Furthermore, the oxygen species play a role in the mechanism of the reaction, favouring the NO_X storage.

Additionally, presence of dopants can reportedly modify the platinum reducibility and platinum-ceria interaction, allowing more readily activation during rich purge.

This project aims to better understand the NO_X storage mechanism on the doped materials and give new insights into the activation/lean deactivation mechanisms in the presence of different dopants.

Objective of this work

The main objective considered in this project is to improve the understanding of the NO_X storage mechanism, together with the mechanism of rich purge on ceria supported platinum. We aim to gain a deeper knowledge of the rich activation and lean deactivation mechanisms as well as determine the structure of the active sites under reaction conditions. We look to develop a method to differentiate between active species and spectator species through transient methods. We will also strive to develop a global kinetic model for the reaction and all involved species. This will enable the determination of the relative importance of different reactions within the catalyst bed as well as a measurement of the exact gas compositional conditions present during the reactions. With this approach in depth information relevant to mechanistic understanding and reaction engineering application will be obtained.

Progress to date

- BET characterisation completed for Nd doped and undoped ceria based catalysts.
- Lean/Rich cyclic experiments completed for Nd doped and undoped ceria based catalysts.
- New catalysts synthesised to include Pr and Sm as dopants for use as publishable alternative dopants.

Conclusions and future work

- NSC tests for all doped and undoped catalysts including new dopants.
- Lean/Rich cyclic experiments for new dopants to compare to Nd effect.
- Characterisation on new dopants.

QUILL Quarterly Report

February 2021 – April 2021

Name:	Sam McCalmont		
Supervisor(s):	Dr Leila Moura, Prof John Holbrey & Prof Margarida Costa Gomes		
Position:	PhD		
Start date:	Jan 2020	Anticipated end date:	2023
Funding body:	EPSRC Doctoral Training Partnership		

Chemisorbent materials for olefin and paraffin separation

Objective of this work

Develop and test new chemisorbent materials for the separation of light olefins and paraffins. In this, achieving high capacity and selectivity for the selected materials. To test this, equipment will be installed, commissioned, and benchmarked for testing under approximate industrial gas stream compositions.

Progress to date

Since the last quarterly report, the commissioning on the gas system, now referred to as the GSS (gas solubility system) has been completed. The GSS used carbon dioxide as the gas for the initial solubility tests. Polyethylene glycol 200 (200 referring to the molecular weight)(PEG200) and 1-butyl-3-methylimidazolium bis(trifluoromethylsulfonyl)imide ([Bmim][NTf_2]) as the initial absorbents. These are shown in Figure 1.

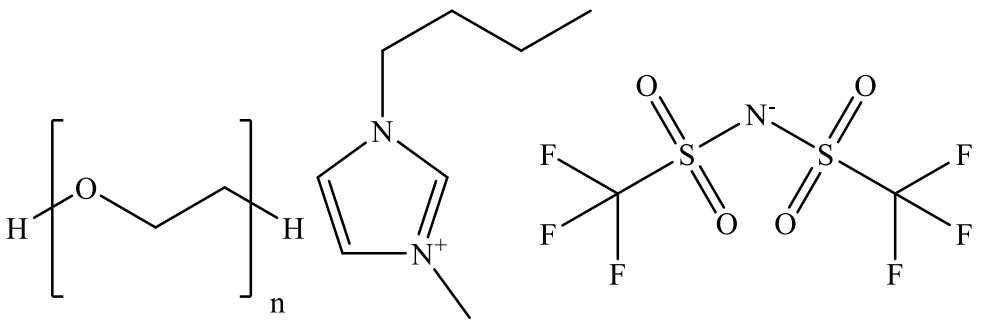

PEG200 [Bmim][NTf2]

Figure 1 - Polyethylene glycol 200 (PEG200) and 1-butyl-3-methylimidazolium bis(trifluoromethylsulfonyl)imide ([Bmim][NTf_2]).

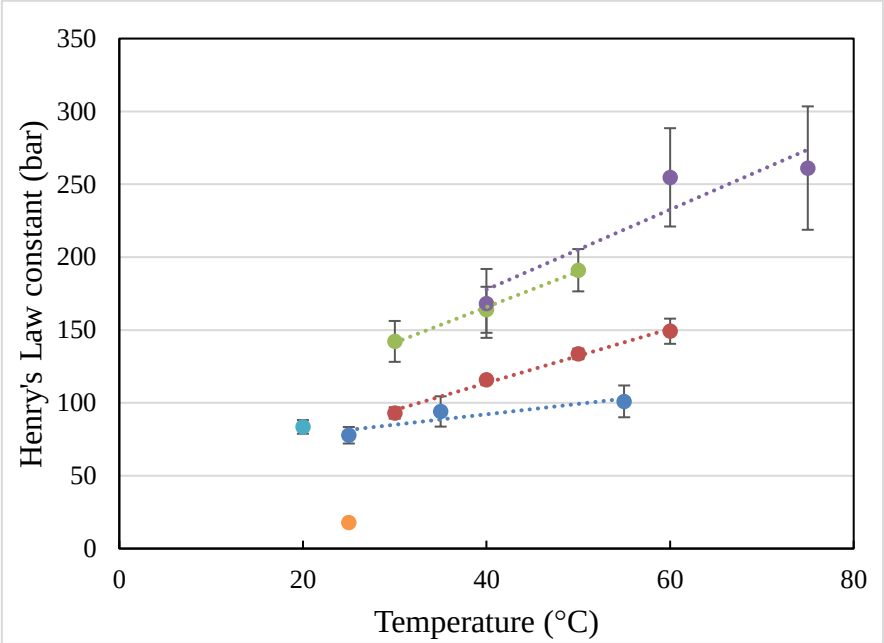

Figure 2 - Henry's Law constant (bar) of carbon dioxide in PEG200 at different temperatures. Initial data compared to other published work (● The GSS, ● Li *et al.,* ● Hou *et al.,* ● Gourgouillion *et al.,* ● Chen *et al.,* and ● Aschenbrenner *et al.*).[1-4]

The solubilities determined from the initial calculations were compared against published work with CO_2 in PEG200.[1-5] The experimental results conducted are shown in Figure 2. The raw data from the published work was taken and converted to be able to compare my work against it. The trend lines are added to show general trend of the data, but not to form a relationship between Henry's Law constant and temperature. The gas system produced viable results. As in as the temperature increased, the solubility of the CO_2 in PEG200 decreased. However, the solubility data collected did not match exactly with what has been published. What can be seen is that there is a difference in what solubility data has been collected, showing that PEG200 may not be the best material to be used. One difference between what has been completed on the gas system compared to other work is the influence of temperature control on the gas. Li *et al.* submerged their equilibrium chamber (CO_2 absorption chamber) fully in a water bath and other components of their apparatus.[1] Li *et al.* equipment best matches that of our gas system.

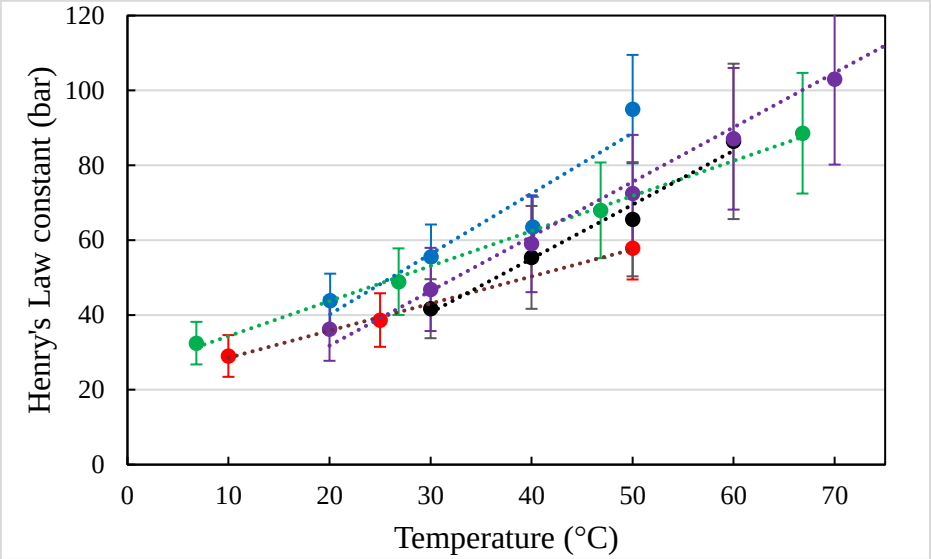

Figure 3 -Henry's Law constant (bar) of carbon dioxide in [Bmim][NTf2] at different temperatures. Initial data compared to other published work (● Bahadur *et al.,* ● Lee *et al.,* ● Anthony *et al.,* ● The GSS and ● Carvalho *et al.*).[1-4]

The next set of tests were completed using [Bmim][NTf_2]. The experiments are being conducted at different pressures and different masses of ionic liquid. The experimental results conducted are shown in figure 3. The results produced on the gas system so far generally lie in the same range as what has been reported.[6-9] The results produced on the gas system are more comparable to the published [Bmim][NTf2] system than the published PEG200 system. This may be down to myself becoming more familiar with the calculations and developing the methodology that allows me to get repeatable values. The raw data from the published work was taken and converted to be able to compare my work against it. The deviation in the Henry's Law constant was also calculated for the published work. The trend lines are added to show general trend of the data, but not to form a relationship between Henry's Law constant and temperature.

The issue that has risen with the results calculated so far is the lack of temperature control, currently the temperature reading coming from the oil bath that the equilibrium chamber is set in. The GSS is being upgraded to replace the equilibrium chamber (as shown in the previous quarterly report) for a mini reactor that will be able to control the temperature and record the temperature of the absorbents in the reactor.

References

1. Li, J.; Ye, Y.; Chen, L.; Qi, Z. *Journal of Chemical and Engineering Data* 2012, **57**, 610–616.
2. Hou, M.; Liang, S.; Zhang, Z.; Song, J.; Jiang, T.; Han, B. *Fluid Phase Equilibria* 2007, **258**, 108–114.
3. Gourgouillon, D.; Nunes Da Ponte, M. *Physical Chemistry Chemical Physics* 1999, **1**, 5369–5375.
4. Chen, Y.; Ma, C.; Ji, X.; Yang, Z.; Lu, X. *Fluid Phase Equilibria* 2020, **504**, 112336.
5. Aschenbrenner, O.; Styring, P. *Energy and Environmental Science* 2010, **3**, 1106–1113.
6. Bahadur, I.; Osman, K.; Coquelet, C.; Naidoo, P.; Ramjugernath, D. *Journal of Physical Chemistry B* 2015, **119**, 1503–1514.
7. Lee, B.-C.; Outcalt, S. L. *Journal of Chemical & Engineering Data* 2006, **51**, 892–897

8. Anthony, J. L.; Anderson, J. L.; Maginn, E. J.; Brennecke, J. F. *The Journal of Physical Chemistry B* 2005, **109**, 6366–6374.
9. Carvalho, P. J.; Alvarez, V. H.; Marrucho, I. M.; Aznar, M.; Coutinho, J. A. *Journal of Supercritical Fluids* 2009, **50**, 105–111.

QUILL Quarterly Report

February 2021 – April 2021

Name:	Anne McGrogan		
Supervisor(s):	Dr Gosia Swadzba-Kwasny		
Position:	PhD		
Start date:	01/10/2019	Anticipated end date:	31/03/2023
Funding body:	EPSRC		

Boron Lewis acids: structure and applications

Background

Boron Lewis acids as co-catalysts for nitrogen activation

I have previously synthesised a wide range of boron compounds and I will explore the use of these boron Lewis acids as co-catalysts for nitrogen activation. Nitrogen is an essential element for all livings things; it has a key role in proteins and nucleic acids, providing the nitrogen content needed to create plants, animals, and other organisms. Biological nitrogen activation by nitrogenase enzymes operates under ambient conditions by employing transition metal-based active sites to bind and reduce the dinitrogen molecule, subsequently releasing it as NH_3 or NH_4^+. While the currently used industrial process requires elevated temperatures and pressures (~500 °C and >100 atm), to combine N_2 and H_2, over an Fe-based catalyst.[1,2] These forcing conditions are required due to the high energy barrier for N_2 triple bond cleavage. The energy requirement to produce NH_3 for fertilisers in the Haber–Bosch process is estimated to be approximately 1.5% of the annual global energy supply.[3] Therefore, more sustainable methods for ammonia synthesis, with reduced energy consumption are desirable.

Introduction to homogenous N_2 activation by Fe^0-based catalysts

The presence of iron in both industrial and biological systems, has led to it being the metal of interest in many dinitrogen activation studies. Even though, N_2 is a poor σ-donor and π- acceptor, many Fe-N_2 complexes have been synthesised with a variety of ligands.[1] The extent of activation of the coordinated N_2 ligand is commonly measured by examining the N-N bond lengths and N–N stretching frequency by IR or Raman spectroscopy.

In 2013, Peters *et al.*[4] reported on several Fe catalysts for the conversion of N_2 to NH_3. They found that catalytic yields of approximately 7 equiv. of NH_3 per Fe could be formed in diethyl ether at −78 °C using the acid $HBAr^F_4$ (46 equiv.) and the very strong reductant KC_8 (50 equiv.) as the proton and electron sources, respectively. In 2017, they reported a significant improvement in yield (80 equiv. NH_3 per Fe) when a significantly weaker combination of reductant (Cp^*_2Co) and acid ($[Ph_2NH_2][OTf]$ was used (Figure 1).[5]

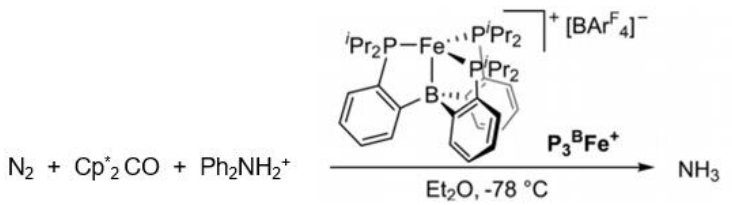

Figure 1 - Summary of the catalytic conversion of N_2 to NH_3 by P_3BFe^+ and the conditions used.

Szymczak *et al.*[6] reported an alternative N_2 activation strategy that is shown to weaken the N-N bond and enhance protonation selectivity through the simple addition of Lewis acids to an Fe(0)-N_2 unit. The idea was to test the "push-pull" hypothesis by which electron density is "pushed" from a reduced iron centre and "pulled" into the N_2 unit by adjacent Lewis acidic sites, thus rendering it more reactive towards protonation. They investigated adducts formed between the iron-dinitrogen complex, [Fe(depe)$_2$(N_2)] (depe=1,2-bis(diethylphosphino)ethane) and several Lewis acids such as $B(C_6F_5)_3$ (**Figure**). From their studies, they reported that the N-N bond strength and N_2 binding affinity can be dramatically tuned by the strength of Lewis acidity, quantified by the acceptor number (AN) (**Figure**).

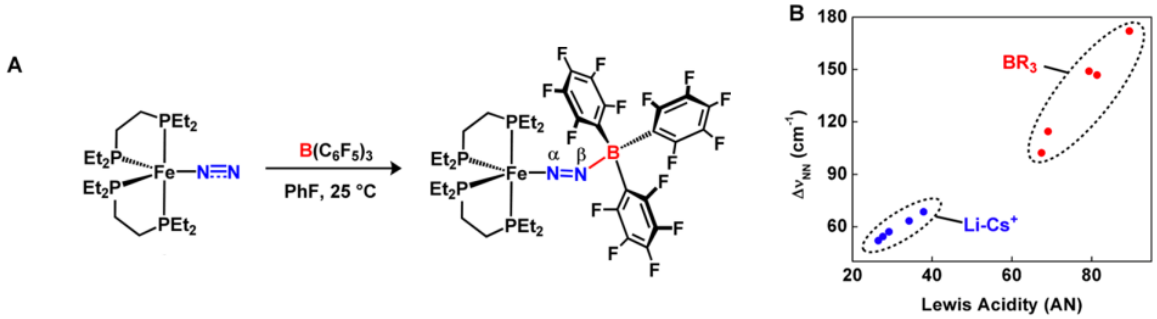

Figure 2 - (A) Formation of adduct between Fe(depe)$_2$(N_2)] and $B(C_6F_5)_3$. (B) Relationship between Lewis acidity and ν_{NN} using a variety of Lewis acids (Li^+, Na^+, K^+, Rb^+, Cs^+; BR_3 (R = 2,6-F_2Ph, 2,4,6-F_3Ph, C_6F_5, OC_6F_5, F)).[6]

Objective of this work

To explore the use of boron Lewis acids as co-catalysts for nitrogen activation.

Progress to date

All manipulations were performed under an atmosphere of dry N_2 using standard Schlenk line techniques, or in an MBraun Labmaster DP glovebox. All glassware was dried at 170 °C overnight before use. Chemicals were obtained from Sigma-Aldrich and used without further purification. Solvents were dried over 3 Å molecular sieves. THF-d_8 was freeze-pump-thaw degassed and dried over 3 Å molecular sieves.

Attempted synthesis of Fe(depe)$_2$$Cl_2$: A solution of depe (0.5 g, 0.00333 mmol) was prepared in 5 mL of DCM and cooled to 0 °C in an ice bath, the solution was then added *via* cannula to a slurry of $FeCl_2$ (0.2 g, 0.00167 mmol) in 10 mL DCM at 0 °C. The solution was stirred at 0 °C for 30 minutes, then allowed to warm to RT and stirred overnight. After filtration, the remaining material was extracted with 5 mL of DCM which was combined with the filtrate. Solvent was removed *in vacuo* and the powder was washed at 0 °C with ethanol (3 x 5 mL) then pentane (5 mL). Awaiting analysis.

I have also been using Dissolve software to analyse neutron scattering data. I have built the model for analysing sulfuric acid and pyridine mixtures. This involved working with Tristan Youngs (the

developer of Dissolve) to incorporate an appropriate force field into the code. I also worked with Tristan as a tester of the software and reported back on bugs, possible improvements, and consistencies between EPSR and Dissolve data. There are still improvements to be made with the code and it is currently in the beta testing phase.

Conclusions and future work

Future work will firstly involve synthesising $Fe(depe)_2(N_2)$ and then testing Lewis acids, including Lewis acidic ionic liquids for N_2 capture. I will also continue to work on analysing neutron scattering data using Dissolve software.

References

1. J. L. Crossland and D. R. Tyler, *Coord. Chem. Rev.*, 2010, **254**, 1883–1894.
2. G. P. Connor and P. L. Holland, *Catal. Today*, 2017, **286**, 21–40.
3. L. Wang, M. Xia, H. Wang, K. Huang, C. Qian, C. T. Maravelias and G. A. Ozin, *Joule*, 2018, **2**, 1055–1074.
4. J. S. Anderson, J. Rittle and J. C. Peters, *Nature*, 2013, **501**, 84–87.
5. M. J. Chalkley, T. J. Del Castillo, B. D. Matson, J. P. Roddy and J. C. Peters, *ACS Cent. Sci.*, 2017, **3**, 217–223.
6. J. B. Geri, J. P. Shanahan and N. K. Szymczak, *J. Am. Chem. Soc.*, 2017, **139**, 5952–5956.

QUILL Quarterly Report

February 2021 – April 2021

Name:	Shannon McLaughlin		
Supervisor(s):	Dr Gosia Swadźba-Kwaśny		
Position:	PhD Student (1st year)		
Start date:	October 2020	Anticipated end date:	July 2024
Funding body:	Department for the Economy		

Thinking inside the (glove)box: Lewis Superacidic Ionic Liquids Based on Main Group Cations

The main aim of this project is to research silicon containing cations as potential components of new Lewis Superacidic ionic liquids. These ionic liquids will have a wide range of applications including use as solvents and catalysts as well well as the extraction of metals and wastes. In this work, the first goal is to synthesise the 'free' trimesitylsilylium cation first isolated by Lambert *et al.*[1]

Synthesis of a 'free' trimesitylsilylium cation:

Synthesis of trimesitylsilane:

Scheme 1: Synthesis of trimesitylsilane.

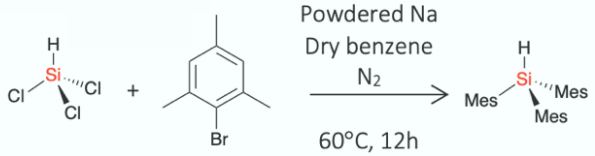

Lappert *et al.*[1]

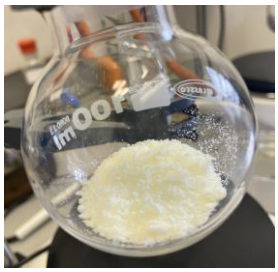

Figure 1- White crystals of trimesitylsilane.

Trimesitylsilylium was synthesised following the method described by Lappert *et al.*[1] 3.02 g of trimesitylsilane (white crystals) was synthesised giving a percentage yield of 38.8%. ^{1}H, ^{13}C and ^{29}Si NMR spectra for trimesitylsilane were recorded, ^{1}H and ^{29}Si NMRs are shown in Figure 2 and Figure 3, respectively. Peaks observed matched exactly to literature values in all NMR spectra.

^{1}H NMR (600 MHz, $CDCl_3$) δ: 2.12 (s, 18H), 2.26 (s, 9H), 5.75 (s, 1H), 6.78 (s, 6H).
^{13}C NMR (600 MHz, $CDCl_3$) δ: 21.14 ppm (p-CH_3), 23.42 ppm (o-CH_3), 128.93 ppm (C_{meta}), 131.23 ppm (C_{para}), 138.96 ppm, (C_{ortho}), 144.80 ppm (C_{ipso}).
^{29}Si NMR (600 MHz, $CDCl_3$) δ: -44.34 ppm.

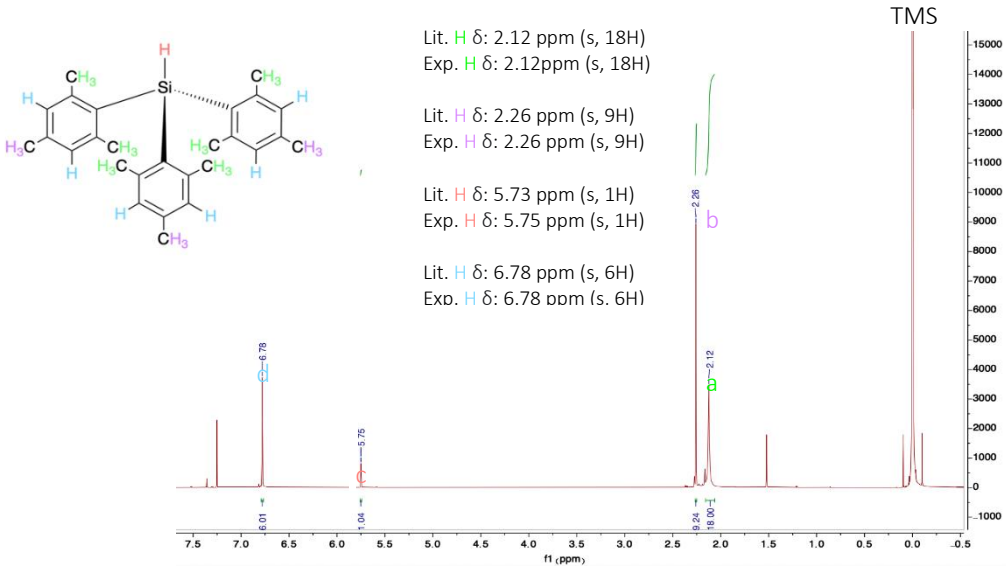

Figure 2 - ^{1}H NMR spectrum of trimesitylsilane in

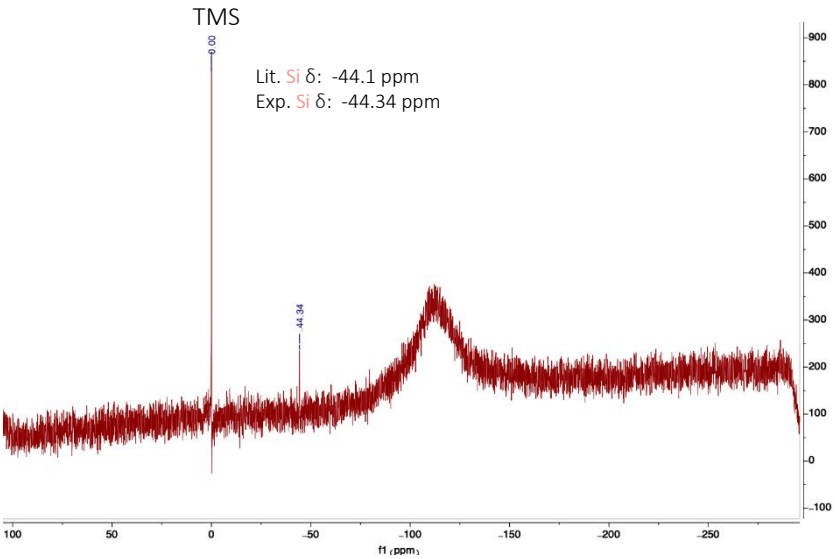

Figure 3 - ^{29}Si NMR spectrum of trimesitylsilane in $CDCl_3$.

Synthesis of chlorotrimesitylsilane:

Scheme 2: Synthesis of chlorotrimesitylsilane.

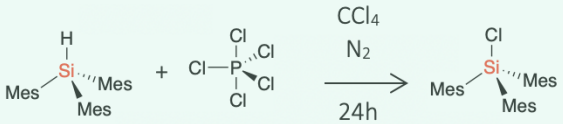

Zigler *et al.*[2]

Chlorotrimesitylsilylium was synthesised following methods described by Zigler *et al.*[2] ^{1}H, ^{13}C and ^{29}Si NMR spectra for chlorotrimesitylsilane were recorded, ^{1}H NMR is shown in Figure 4. Excess peaks were present due to impurities and solvents. Methanol appears as a singlet at 3.49 ppm and hexane appears as a triplet at 0.88 ppm and a multiplet at approximately 1.26 ppm. There is also a small amount of starting reagent remaining at 5.75 ppm. The reaction mixture will be refluxed again until no starting reagent can be detected and then dried thoroughly on the Schlenk line to remove the solvent impurities.

^{1}H NMR (600 MHz, $CDCl_3$) δ: 1.96 – 2.46 (br, 18H), 2.24 (s, 9H), 6.72 – 6.90 (br, 6H).
^{13}C NMR (600 MHz, $CDCl_3$) δ: 20.02 ppm (p-CH_3), 23.97 ppm (o-CH_3), 127.88 ppm (C_{meta}), 131.92 ppm (C_{para}), 138.66 ppm (C_{ortho}), 143.75 ppm (C_{ipso}).

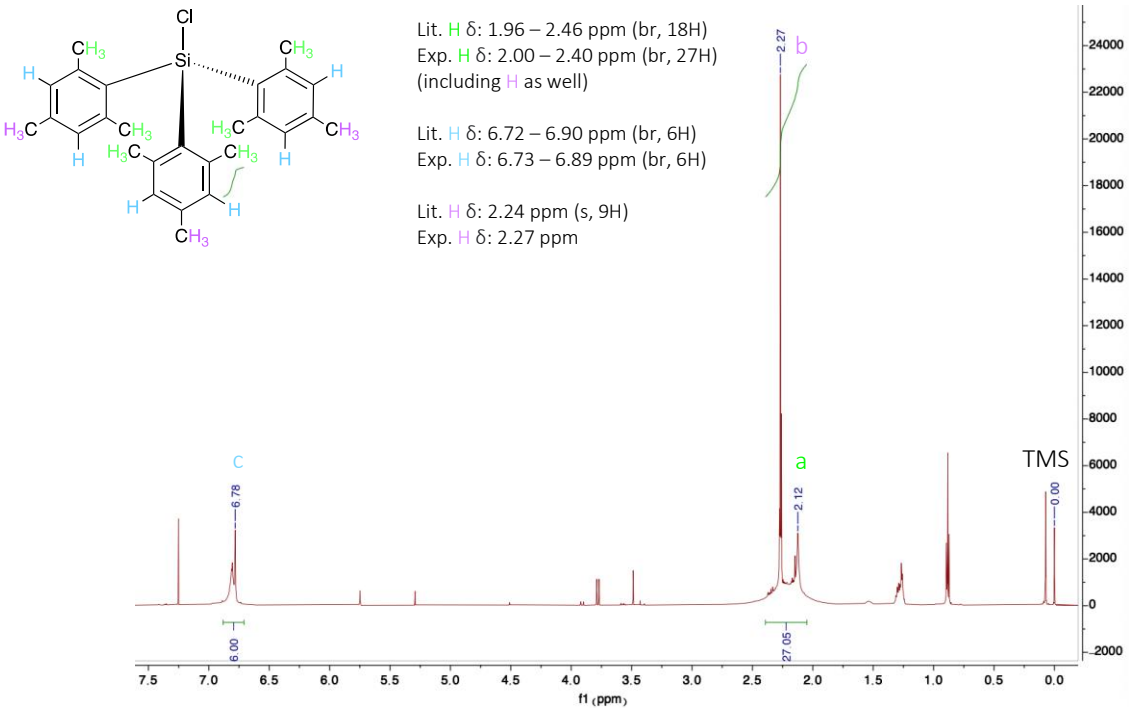

Figure 4 - ^{1}H NMR spectrum of chlorotrimesitylsilane in $CDCl_3$.

Hydrogenation Splitting using FLPs:
160 mmol solutions of three different FLPs were made up in *d_6*-benzene, [C_2mim][NTf_2] and [C_{10}mim][NTf_2]. The phosphorus compounds chosen to make up the FLPs were tri-*tert*-butylphosphine, trioctylphosphine and diphenyl(pentafluorophenyl)phosphine (Figure 6).

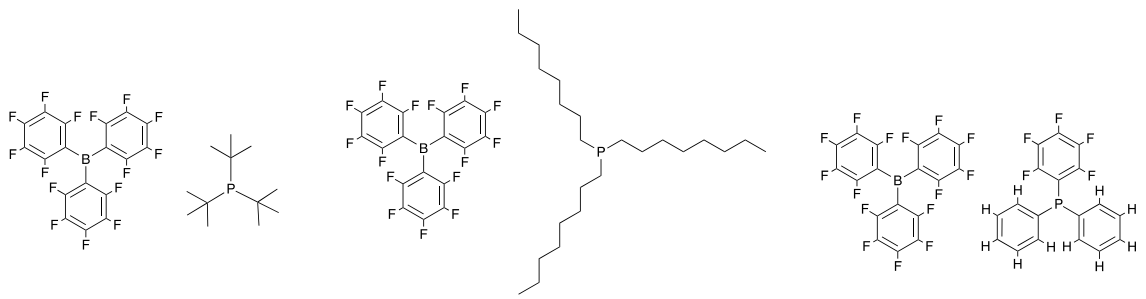

$B(C_6F_5)_3/P(^tBu)_3$ $B(C_6F_5)_3/P_{888}$ $B(C_6F_5)_3/P(C_6F_5)Ph_2$

Figure 5 - Structure of FLPs under investigation.

These FLP were investigated for their ability to split hydrogen. A novel NMR tube, illustrated in Figure 3, was designed with a wider neck allowing a septum to be attached and two needles connected. This setup allows H_2 to be bubbled through the FLP in d_6-benzene/ionic liquid directly in the NMR tube. Pure hydrogen was bubbled through the FLP solutions at a rate of 2 ml/min for 12 hours. Table 1 illustrates which FLP systems were able to successfully split hydrogen. Uptake of hydrogen was confirmed by the formation of a new pair of broad peaks of equal integration in the ^{1}HNMR. When hydrogen was bubbled through $P(^tBu)_3/B(C_6F_5)_3$ in d_6-benzene the d_6-benzene evaporated through the outlet needle. Therefore, the other two d_6-benzene samples could not be hydrogenated using this setup.

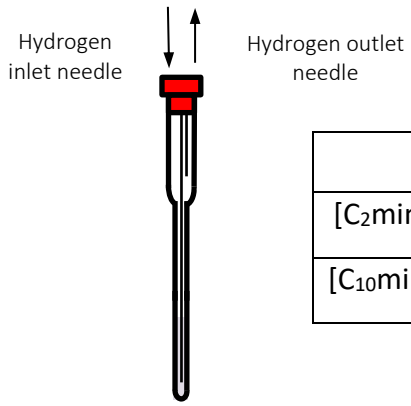

	$B(C_6F_5)_3/P(^tBu)_3$	$B(C_6F_5)_3/P_{888}$	$B(C_6F_5)_3/P(C_6F_5)Ph_2$
$[C_2mim][NTf_2]$	✓	✓	✗
$[C_{10}mim][NTf_2]$	✓	✓	✗

Table 1 - Table showing which FLP systems were able to successfully split hydrogen ✓ and which ones could not ✗.

Figure 6 - Diagram of hydrogenation setup.

Synthesis of Ionic Liquids:

Trihexyl(tetradecyl)phosphonium chloride $[P_{66614}]Cl$ was converted to either trihexyltetradecyl-phosphonium tetrafluoroborate ($[P_{66614}][BF4]$) or trihexyltetradecyl-phosphonium thiocyanate ($[P_{66614}][SCN]$) *via* an anion exchange reaction (Scheme 4). Synthesis was conducted on 50 g scale for each ionic liquid. Both ionic liquids were washed initially with a deionised water salt solution and DCM. 10 -15 subsequent washes were performed with the corresponding deionised water and salt solution. Solutions were tested with silver nitrate solution and XRFs were taken until no chloride anions were remaining. Trihexyl(tetradecyl)phosphonium tricyanomethane ($[P_{66614}][TCM]$) will also be synthesised on a 50 g scale *via* this method. $[P_{66614}][BF_4]$, $[P_{66614}][SCN]$ and $[P_{66614}][TCM]$ will be utilised in a collaborative study with the Wojnarowska group.[3] This group classifies ionic liquids under extreme pressure and studies phase transfer as a function of pressure instead of temperature.

Scheme 4 - Synthesis of $[P_{66614}][BF_4]$, $[P_{66614}][SCN]$ and $[P_{66614}][TCM]$.

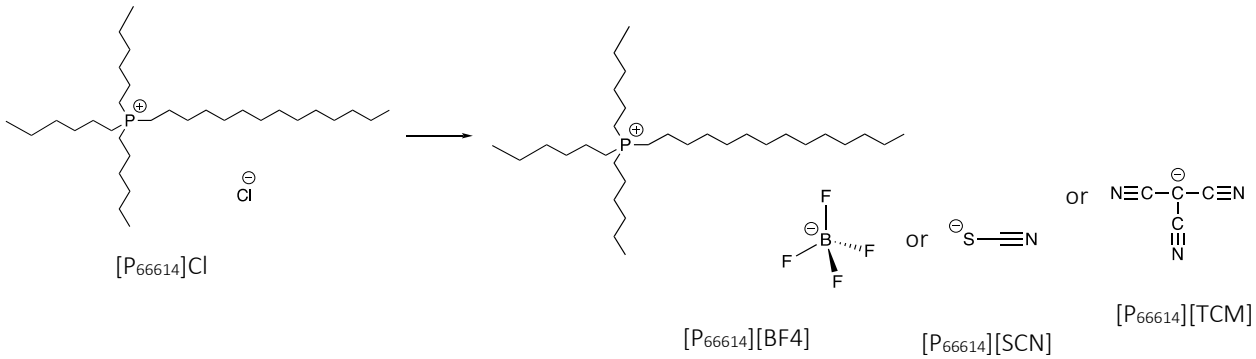

Future Work:

Synthesis of trimesitylsilane:
Future work will involve completing the final two steps of the proposed synthesis of the 'free' trimesitylsilylium cation.

Allyltrimesitylsilane and trimesitylsilylium tetrakis(pentafluorophenyl)borate (compound 1) will be synthesised following methods described by Lambert *et al.*[4] and Lambert and Zhao[5] respectively. After compound 1 has been successfully synthesised, it will be combined with commonly used anions such as $[NTf_2]^-$ and $[FSI]^-$ to conduct characteristic studies of the cation.

Scheme 5: Synthesis of allyltrimesitylsilane.

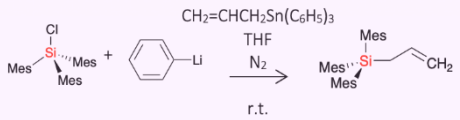

Lambert *et al.*

Scheme 6: Synthesis of a 'free' trimesitylsilylium cation.

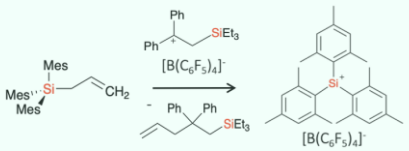

Lambert and Zhao.

1

The next aim would be to combine the trimesitylsilylium cation with borate anions or cyanoborate anions in hope of generating new Lewis superacidic ionic liquids. Applications of these newly developed ionic liquids will then be investigated for potential use as solvents and catalysts.

Potential Anions:

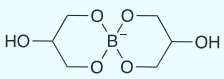

Borate anion
$Na[BX_n(CN)_{4-n}]$
X = alkyl
Cyanoborate anions

Target Cation:

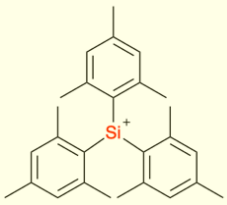

'Free' trimesitylsilylium cation

Figure 7- Structure of the target trimesitylsilylium cation and potential borate anions or cyanoborate anions.

Hydrogenation Splitting using FLPs:
The FLP/IL mixtures mentioned previously will be used in two areas of research.

Hydrogenation of Organic Substrates:
The first area of research involves an ongoing study into frustrated Lewis pair catalysis in ionic liquids. The FLP systems that successfully split hydrogen will be used to hydrogenate organic substrates. 1,1-diphenylethylene was chosen as the first substrate to be investigated as it has been previously observed to be effectively reduced by FLP systems[6,7] (Scheme 7). 0.1 ml of 1,1-diphenylethylene will be added to each FLP system and pure hydrogen will be bubbled through the FLP solutions at a rate of 2 ml/min for 12 hours. The progress of hydrogenation will be monitored using ^{1}H, ^{13}C, ^{19}F, ^{31}P and ^{11}B NMR spectroscopy.

Scheme 7 - Reduction of 1,1-diphenylethylene to 1,1-diphenylethane.

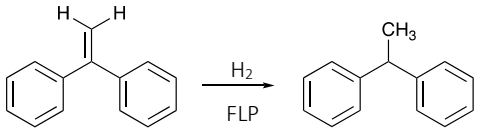

Collaborative Studies:
The second area of research utilises the FLP/IL systems as potential electrolyte media for hydrogen detection. Previous studies into room temperature ionic liquids (RTILs) have shown promise as potential air stable and non-volatile electrolytes for amperometric gas sensors.[8-10] 0.5ml samples of $[C_2mim][NTf_2]$, $P(^tBu)_3/B(C_6F_5)_3$ in $[C_2mim][NTf_2]$ before hydrogenation and $P(^tBu)_3/B(C_6F_5)_3$ in $[C_2mim][NTf_2]$ after hydrogenation will be sent to the Silvester[9] research group for further investigation.

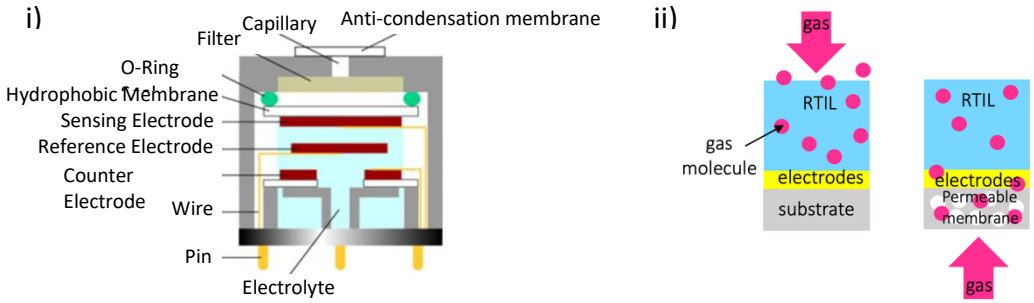

Figure 8 - Schematic diagrams of i) the structure of an amperometric gas sensor ii) diffusion of gas molecules from gas phase through IL to the electrode.

References

1. M. Gynane, M. Lappert, P. Riley, P. Rivière and M. Rivère-Baudet, Journal of Organometallic Chemistry, 1980, 202, 5-12
2. S. Zigler, L. Johnson and R. West, Journal of Organometallic Chemistry, 1988, 341, 187-198.
3. M. Musiał, S. Bair, S. Cheng, Z. Wojnarowska and M. Paluch, *J. Mol. Liq.*, 2021, **331**, 115772.
4. J. B. Lambert, C. L. Stern, Y. Zhao, W. C. Tse, C. E. Shawl, K. T. Lentz and L. Kania, *J. Organomet. Chem.*, 1998, **568**, 21–31
5. K. C. Kim, C. A. Reed, D. W. Elliott, L. J. Mueller, F. Tham, L. Lin and J. B. Lambert, *Science.*, 2002, **297**, 825–827.
6. L. Greb, P. Oña-Burgos, B. Schirmer, S. Grimme, D. W. Stephan and J. Paradies, *Angew. Chemie – Int. Ed.*

7. S. Tamke, C.G. Daniliuc and J. Paradies, *Org. Biomol. Chem.*
8. E. I. Rogers, A. M. O'Mahony, L. Aldous and R. G. Compton, *ECS Trans.*, 2019, **33**, 473.
9. D. S. Silvester, *Curr. Opin. Electrochem.*, 2019, **15**, 7–17.
10. I. Cretescu, D. Lutic and L. R. Manea, in *Electrochemical Sensors Technology*, InTech, 2017.

QUILL Quarterly Report

February 2021 – April 2021

Name:	Hugh O'Connor		
Supervisor(s):	Prof Peter Nockemann & Dr Stephen Glover		
Position:	PhD Student		
Start date:	October 2019	Anticipated end date:	June 2023
Funding body:	EPSRC		

Redox Flow Battery Materials for Energy Storage

Results from research into the performance of 3D-printed Redox Flow Battery cells have been written up, and a thorough examination into different 3D-printed polymers and their use in flow battery production has been carried out. The cell design has been further optimised, along with the materials used to ensure leak prevention and ease of use. Work is currently ongoing into the experimental graphene nanocomposite polymers and their use in 3D-printing of flow batteries. Using the 3D-platform developed throughout this quarter, work is beginning on the investigation of new flow battery topologies to improve the power density of flow battery cells. Furthermore, an investigation into 3D-printing flow electrochemistry devices using polypropylene is also being carried out based on findings from previous studies.

QUILL Quarterly Report

February 2021 – April 2021

Name:	**Scott Place**		
Supervisor(s):	Dr Paul Kavanagh (Principal) & Dr Mark Muldoon (Secondary)		
Position:	PhD Student		
Start date:	10/19	Anticipated end date:	07/23
Funding body:	DfE		

Copper Based Electrocatalysis for Energy Applications and Sensing

Due to COVID, I made the decision to take a leave of absence for 4 months beginning in February of this year (2021). I returned to work at the beginning of June. As such, no progress was made on my PhD project during the period of February-April; the next report will present a summary of work completed from June.

QUILL Quarterly Report

Feb 2021 - Apr 2021

Name:	Yaoguang Song		
Supervisor(s):	Prof Peter Nockemann & David Rooney (QUB), Dr Xiaolei Zhang (Strathclyde), Prof Stuart Gibb & Dr Szabolcs Pap (UHI)		
Position:	PGR Student		
Start date:	3rd Dec 2018	Anticipated end date:	31 Dec 2021
Funding body:	EU INTERREG VA Programme, managed by SEUPB		

Thermochemical Conversion of Biomass Lignin into Mesoporous Carbon Materials

Background

As a main component, lignin from biomass holds huge potential for producing mesoporous carbons (MCs)[1,2,3], which represents upper-class valuable products amongst all lignin-based applications.[4] However, most preparation methods for MCs are empirical, leading to unpredictable topologic and structural properties thus likely unfavourable for aimed downstream applications. Soft-templating synthesis was reported successful to tune nanostructures effectively, but novel promising templates are still in need of development.

A good option is long-chain ionic liquids (ILs) comprised of solely ions, as they can form lyotropic liquid crystals (LLCs), micelles, and (micro) emulsions that have been used for templating synthesis as well. Besides, ILs are also increasingly seen in the dissolution and depolymerisation of lignin. Therefore, this programme aims to investigate the possibility to convert lignin into MCs by employing ILs as both structure-directing agent and solvent. The effective implementation involves both multiscale modelling for computational design of preparation method and tangible experimental validation.

My last quarterly report introduced the coarse-grained (CG) molecular dynamics (MD) simulations to investigate how the third chemical species influence the self-assembly of ternary mixtures containing IL template, phenolic compounds as precursor, and water. Results indicate that the increasing hydroxyl groups in precursor influence both the morphologies of IL template and the distribution of phenolic compounds themselves. As shown in Fig 1, the morphologies of mixtures with different precursor at the same mixing ratio are different. Some of the experimental validation work such as polarised optical microscopy (POM), have been reported previously. In this report, more work will be included, from the distribution analysis to the validation of simulation results, especially the distribution of phenolic precursors in ternary mixtures. 2D NOESY NMR and density functional theory (DFT) calculations are employed as useful validation techniques.

Results

Polymer precursor – IL templates spatial correlation analysis

In practical templating synthesis of porous polymer/carbon materials, precursors are expected to be attached to then cross-linked in the amphiphilic part of the templates.[5–7] Therefore, we studied how various precursors were distributed in templates-containing mixtures.

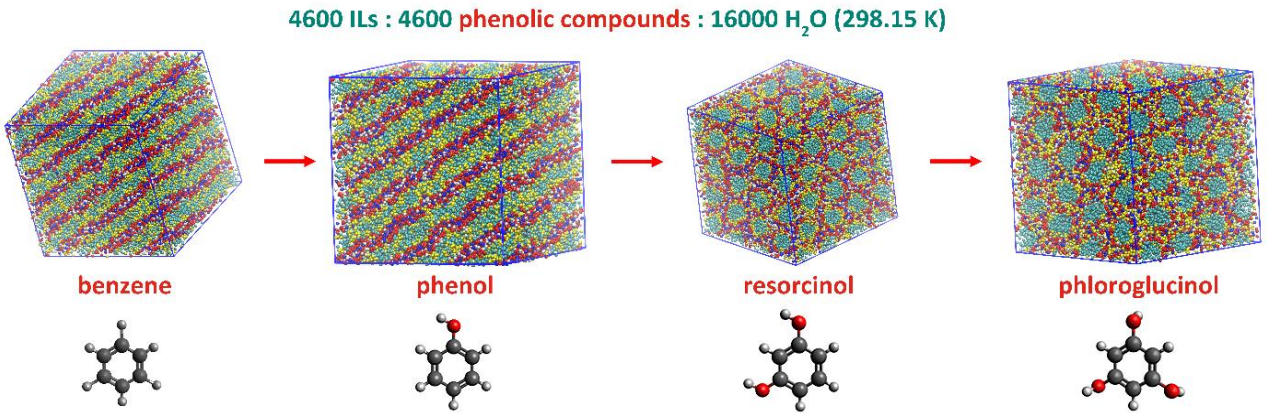

Figure 4 - Morphology evolution under increasing hydroxyl groups in phenolic compounds (Red: imidazolium ring, cyan: alkyl chain, blue: acetate anion, yellow: phenolic compounds, white: water)

CGMD simulation results in Fig 1 highlighted the spatial differences of various phenolic compounds. It is noticeable that molecules of phenol (yellow particles), as well as benzene, were mostly seen in the hydrophobic phase formed by the aggregation of chains on the cations (cyan particles); resorcinol and phloroglucinol were dispersed toward the outer layer of micelles, the aqueous phase. This infers that the addition of chemical species influenced not only ILs morphology during self-assembly, but also the position of these molecules within the multi-phase system.

Centre of mass (COM) radial distribution functions (RDF) showed that anion-water pair was the most prominent correlation within all the four ternary systems (Fig 2). This is most likely related to the strong H-bonding interaction between acetate and water. $-COO^-$ are expected to form 6 H-bonds with water molecules on the average.[8] For ternary mixtures containing benzene or phenol, the subsequent strongest correlations were cation-anion and cation-water pairs (Fig 2a and b). Both benzene and phenol showed the weakest correlation preference to both ILs and water. With the growth in hydroxyl number, the peaks for resorcinol-anion correlation and resorcinol-water correlation grow higher, leaving cation-resorcinol correlation as the weakest (Fig 2c). Fig 2d shows

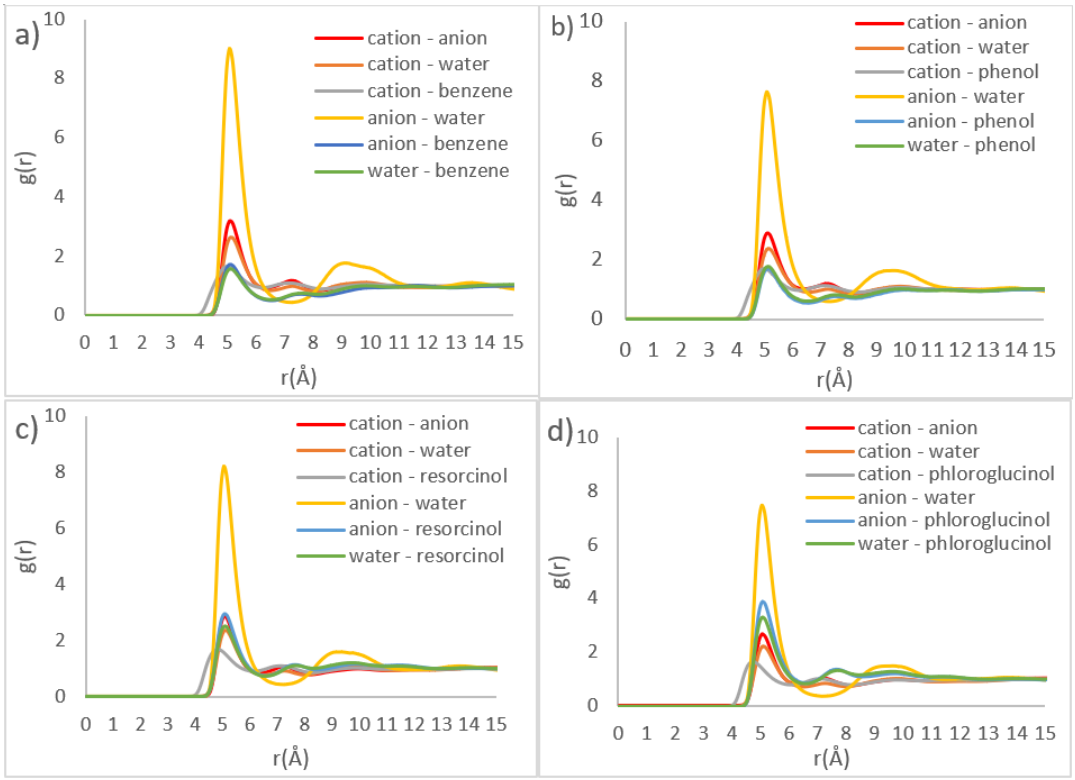

Figure 5 - COM RDFs for ternary systems containing a) benzene, b) phenol, c) resorcinol, and d) phloroglucinol, respectively

the COM RDF analysis of ternary mixture containing phloroglucinol. The correlation between phloroglucinol and acetate anion becomes the second strongest, followed by phloroglucinol-water pair. The introduction of more hydroxyl groups to polymer precursors favours the interaction between precursor and aqueous phase.

The detailed site-site RDFs between phenolic precursors and IL cation were analysed and shown in Fig 3. Phenol has the strongest correlation with bead cation 4, followed by cation 5 and 6 (Fig 3b). This indicates phenol has a particular distributional preference towards alkyl chains, especially the area where the alkyl chain attaches to the imidazolium ring. Similar tendency was also found in the case of benzene. However, the interactions between resorcinol and the imidazolium ring of the cation become stronger, whereas the correlation for cation 4-resorcinol pair remains the strongest (**Error! Reference source not found.**c). Compared with phenol, the two hydroxyl groups in resorcinol double its H-bonding ability. Consequently, resorcinol was dispersed mostly around the imidazolium ring where there is a higher possibility to interact with acetate and water via H-bonds. As shown in **Error! Reference source not found.**d, when the hydroxyl number tripled, the strongest site-site correlations were found in phloroglucinol-cation 1 and phloroglucinol-cation 2 pairs, as opposed to cation 4 as witnessed previously. Since phloroglucinol was completely dispersed into the hydrophilic

phase, the outer layer of template clusters, the correlation between phloroglucinol and the alkyl chain became the weakest.

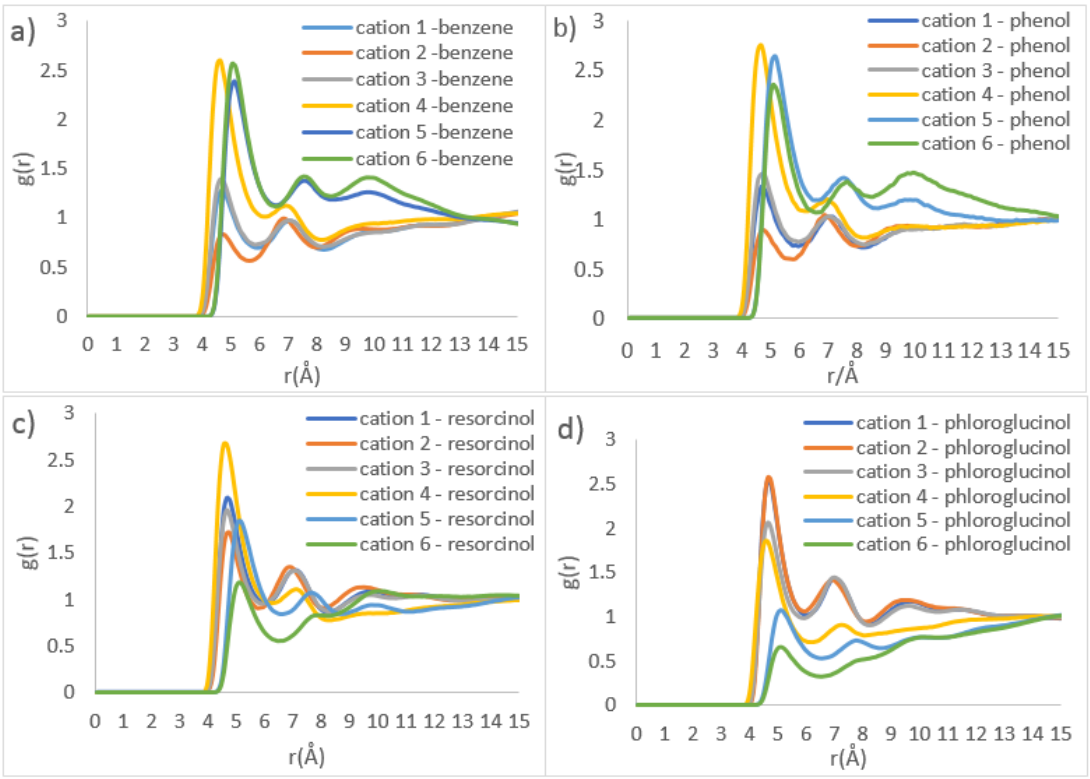

Figure 6 - Site-site RDFs of IL templates and various precursors a) benzene, b) phenol, c) resorcinol, and d) phloroglucinol, respectively.

Structural optimisation via DFT calculation

Based on the RDF analyses, it seems that involving more hydroxyl moieties in the precursor favours the interaction with the amphiphilic part of template, leaving the hydrophobic part as pore structures. To confirm this, the structures of ternary mixtures containing a single ion pair were optimised by DFT calculations to manifest the dominant configurations within the dynamic systems. As shown in **Error! Reference source not found.**, benzene and phenol have the least distance with C5-C7, C2-C5 of the alkyl chain, respectively. Resorcinol is distributed around C1 and C2, and phloroglucinol at N atom linked to the methyl side group of the cation. The distance between terminal carbon and the projection point of polymer geometric centre onto the alkyl chain was calculated as a reference to show the degree of diffusion. It is evident that the reference distance becomes larger from benzene to phloroglucinol with the increasing hydroxyl groups. This result coincides well with the strongest pair spatial correlations in CGMD simulations.

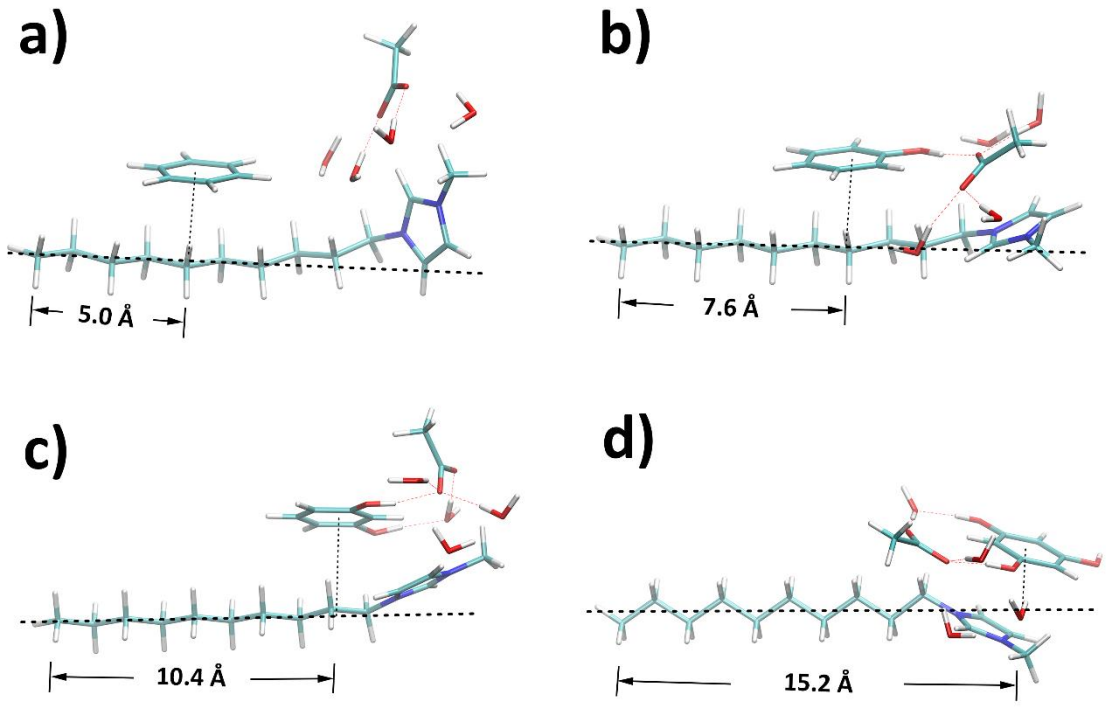

Figure 7 - Structures optimised by DFT for ternary mixtures containing a) benzene, b) phenol, c) resorcinol, and d) phloroglucinol, respectively.

Experimental validation

Experimental evidence was also obtained by 2D NOESY NMR technique. Protons close to each other in space with distance less than 3.5 Å are likely to show stable cross peaks in the 2D spectra. NOESY experiment for benzene-based ternary mixture was performed with deuterated oxide as internal reference due to the formation of lyotropic gels. From **Error! Reference source not found.**, the protons on benzene (7.0 ppm) only showed cross peaks with H atoms linked to C3-C9 in the alkyl chain (broad peak from 0.9 to 1.0 ppm) therefore benzene is mostly distributed near alkyl chain. As aforementioned, benzene barely interacts with ILs and water so non H-bonding interactions like hydrophobic interaction play the major roles in the distribution of benzene. H atoms on phenol (6.5, 6.3, and 6.1 ppm) also showed weak cross peak with methyl group linked to the imidazolium ring, which infers that a small proportion of phenol remain in aqueous phase during the dynamic process. The cross peaks between protons on resorcinol (6.2, 5.8, and 5.7 ppm) and imidazolium ring (6.7 and 6.6 ppm) confirm that resorcinol had started to disperse into the aqueous phase. When the hydroxyl groups are tripled, strong cross peaks from the resulting interactions between phloroglucinol (5.0 ppm) and aqueous phase (mainly water at 6.0 ppm and acetate at 1.1 ppm) were also observed; this indicated phloroglucinol has been dispersed into the hydrophilic aqueous phase. Moreover, another noticeable phenomenon is that the peak for water shifted to high field with the growing hydroxyl group number in phenolic compounds, from 5.5 ppm in phenol case to 6.0 ppm in phloroglucinol case, which is also resulted from the stronger H-bonding interaction between polymer precursor and water.

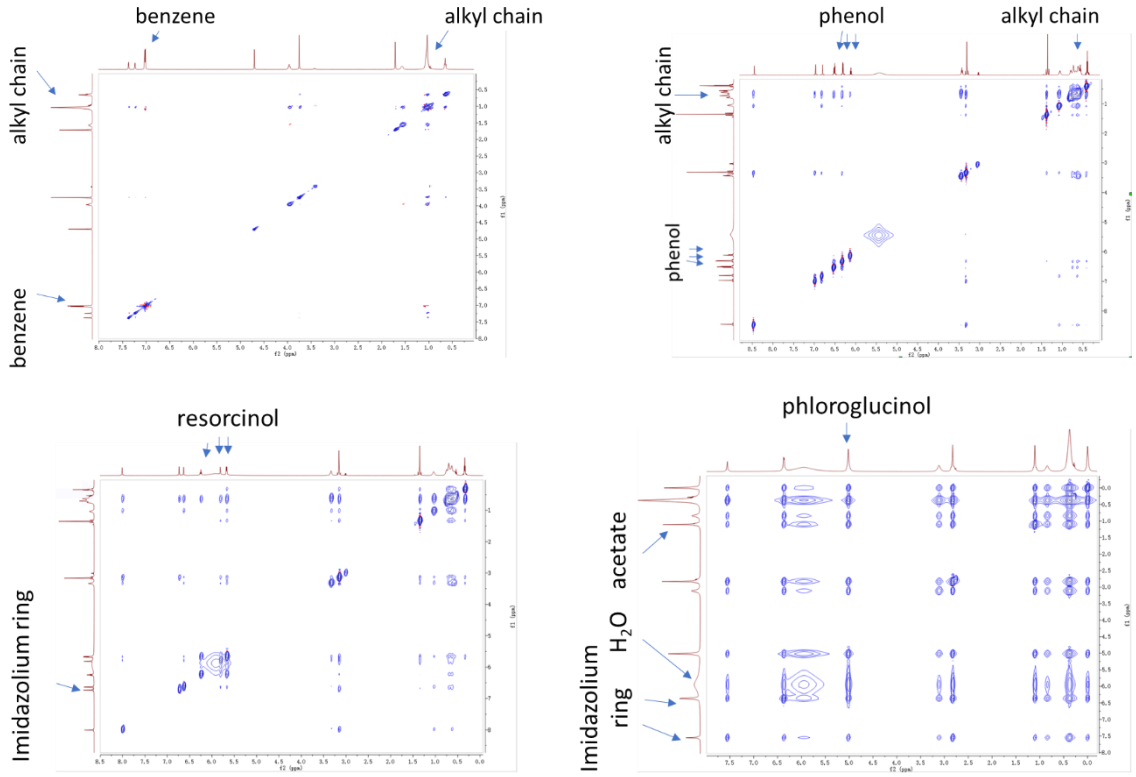

Figure 8 - 2D NOESY experiments for ternary mixtures containing a) benzene, b) phenol, c) resorcinol, and d) phloroglucinol

Conclusions and future work

The influence of hydroxyl groups in phenolic precursor on the template-precursor spatial correlation was investigated by CGMD simulation, DFT calculation, and 2D NOESY NMR experiments. Results showed excellent coincidence. To validate the morphological evolution, small-angle X-ray scattering technique is under performing. In the future, carbon materials will be prepared with the guidance of modelling results. Related characterisation will also be performed to study the carbon materials based on simulation if appropriate.

References

1. D. Montané, V. Torné-Fernández and V. Fierro, *Chem. Eng. J.*, 2005, **106**, 1–12.
2. Y. Song, J. Liu, K. Sun and W. Xu, *RSC Adv.*, 2017, **7**, 48324–48332.
3. J. M. Rosas, R. Berenguer, M. J. Valero-Romero, J. RodrÃ-guez-Mirasol and T. Cordero, *Front. Mater.*, , DOI:10.3389/fmats.2014.00029.
4. A. M. Puziy, O. I. Poddubnaya and O. Sevastyanova, *Top. Curr. Chem.*, 2018.
5. C. Liang, Z. Li and S. Dai, *Angew. Chemie - Int. Ed.*, 2008.
6. D. Saha, R. Zacharia and A. K. Naskar, in *ACS Symposium Series*, 2014.
7. Y. Meng, D. Gu, F. Zhang, Y. Shi, L. Cheng, D. Feng, Z. Wu, Z. Chen, Y. Wan, A. Stein and D. Zhao, *Chem. Mater.*, 2006, **18**, 4447–4464.
8. M. V. Fedotova and S. E. Kruchinin, *J. Mol. Liq.*, 2011, **164**, 201–206.

QUILL Quarterly Report

Feb 2021 – Apr 2021

Name:	Richard Woodfield		
Supervisor(s):	Dr Stephen Glover, Dr Robert Watson & Prof Peter Nockermann		
Position:	PhD Candidate		
Start date:	06/2019	Anticipated end date:	12/2022
Funding body:	EPSRC		

Modelling the use of Flow Batteries in Transport Applications

Background

Flow batteries have received significant attention in the past years for use in grid storage applications. The decoupling of the relationship between power and energy density offers a very unique way to store energy to suit the user's particular needs. The extremely long cycle life of a flow-battery is another attractive asset, as the electrodes do not undergo cyclic stressing in the same way Li-ion and other chemistries do. Flow-batteries have received very limited attention regarding their use in transport applications. There is untapped potential in the fact that the discharged electrolyte of a flow-battery could be rapidly swapped at a traditional gas-station, where the infrastructure is already half in-place with storage tanks under the stations. With the electrolyte being entirely re-usable, the station would use an on-site flow-battery to recharge their reservoir and provide passing vehicles with opportunity to swap their electrolyte with readily charged fluid.

Objective of this work

The overall goal of the project is to identify viable electric or hybrid modes of transport that would benefit from the use of a flow-battery, given the refillable nature of the flow-battery electrolyte reservoirs. Even the applications rendered not viable will have outcomes, as the amount by which the energy density of the electrolyte would need to improve by is also providing electrolyte chemists with targets to aim for. The investigations will be carried out using software to model battery and vehicle behaviour, primarily Simulink.

Progress to date

Modelling work has shown that coastal ferries are a very good candidate for RFB technology, and a paper has been submitted in this area.

Conclusions and future work

Modelling work is now shifting towards bus applications, exploring a range of system architectures and control strategies.

QUILL Quarterly Report

February 2021 – April 2021

Name:	John (Mark) Young		
Supervisor(s):	Dr Leila Moura, Prof John Holbrey and Prof Sophie Fourmentin		
Position:	PhD student		
Start date:	2020	Anticipated end date:	2024
Funding body:	EPSRC		

Gas separation technologies

Background

Biogas is a renewable and carbon neutral energy source obtained through anaerobic digestion (AD) of organic waste. Biomethane is obtained through the upgrading of biogas produced from anaerobic digestors. It consists of mainly methane and carbon dioxide with many trace compounds including hydrogen sulfide, ammonia, silioxanes, terpenes and water vapour. Biomethane must be of a purity equal to or better than that of natural gas if it to be utilised for grid injection therefore a methane purity of above 96% must be achievable form any prospective technology. Carbon dioxide should make up 2.5-4% of the remaining volume with contaminants such as sulfer and siloxanes being limited to 10 mg/m^3 and 0.1 mg/m^3 respectively. Due to the major biogas components being carbon dioxide and methane it is this separation we will focus on in this project.[1]

Currently biogas upgrading is multistep and scrubbing is mainly used for carbon dioxide and methane separation. This involves the use of liquid amines where the carbon dioxide uptake occurs through a chemisorption process. This requires high energy for amine regeneration in the form of steam at 100-150^{o}C to reform the initial liquid amine. Water scrubbing can also be used but this requires vast amounts of water and leads to methane slip due to the lower selectivity of water compared with other technologies. Membranes offer another option for upgrading but these also suffer from a range of issues such a low throughput coupled with fouling and plasticisation. The degradation of membranes leads to issues both economically in the form of having to replace them but from an environmental standpoint it is unsustainable to continuously have to dispose of and manufacture replacement membranes. Cryogenic distillation offers a method of using nontoxic materials to produce high purity gas streams through the utilisation of low temperatures and high pressures which allows carbon dioxide to liquify leaving a pure methane stream. However the energy cost associated with this method is massive which makes it less sustainable and exceedingly costly.[2]

It is for these reasons that we seek to create a novel materials which will be more efficient, more sustainable and economically viable. Initial work will consist of the use of deep eutectic solvents in conjunction with other sorbents to increase their upgrading capabilities.

Work to date

The HS-GC screening methodology has been my major focus since the last report and has improved considerably. Calibration curves for both CO_2 an CH_4 have been completed giving R^2 values > 0.995 which shows direct correlation between GC peak area and initial pressure as can be seen in figure 1. This was achieved through the use of correct vial components so as to full reseal the vial after

puncture with a 23 gauge needle. Much testing and methodology development was carried out in order to achieve these results including the testing of many vial components and HS-GC method alterations.

Figure 1 also shows equilibrated samples with [Bmim][NTf_2] which from literature we know should have a high CO_2 capacity[3] and low CH_4 capacity.[4] These samples were plotted using initial pressure injected into the vial where variation in the peak area is attributed to the sample. The Peak area of what we expect from the calibration curves of CO_2 is substantially higher than what we see with equilibrated samples. This indicated that differences are attributed to gas uptake by the ionic liquid when we consider control vials remain on the calibration curves after being allowed to equilibrate for the same amount of time. This rules out leaks as a possible source of peak area decrease. As expected the equilibrated sample with CH_4 shows almost no change when compared with the calibration curve.

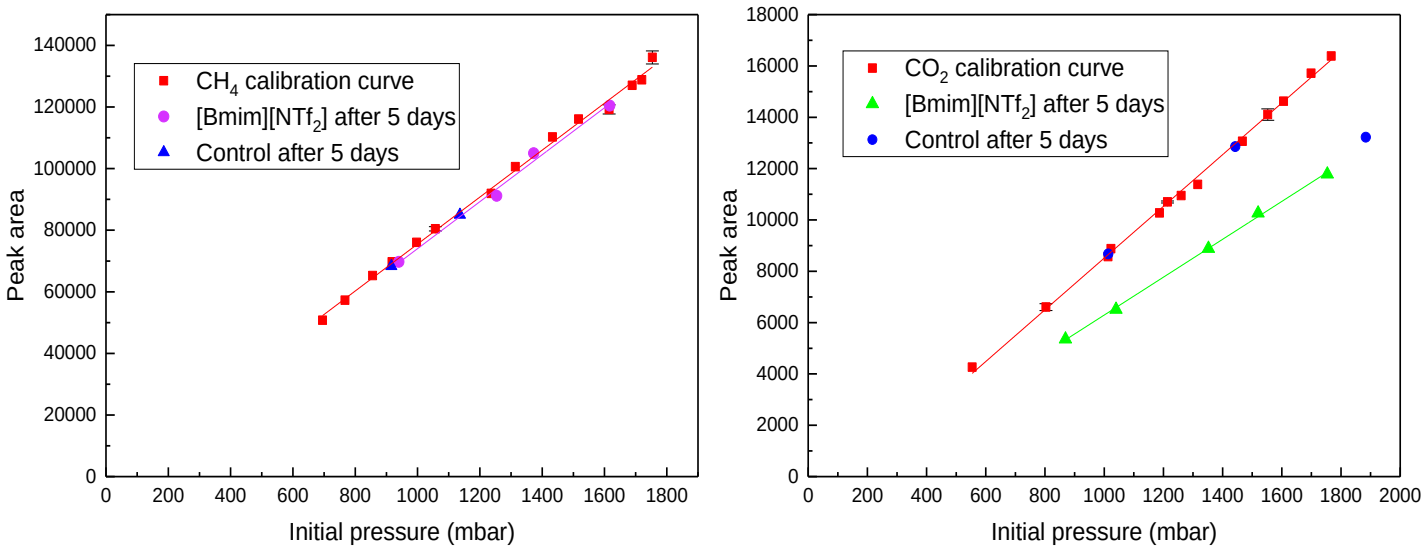

Figure 1 - Calibration curves with both CO_2 (left) and CH_4 (right) along with first material testing of [Bmim][NTf_2] with both gasses

It was also found that the maximum pressure that this testing can be carried out at is around 1800 mbar (figure 2). This was initially though to be due to septa leaks but more recently it has been found that different septa are following the exact same trend. These septa can be viably seen holding pressure up to 3 bar with no leaks. This indicated that the GC is limiting maximum pressure. We hope to in future carry out experiments with our own HS-GC to alleviate this issue.

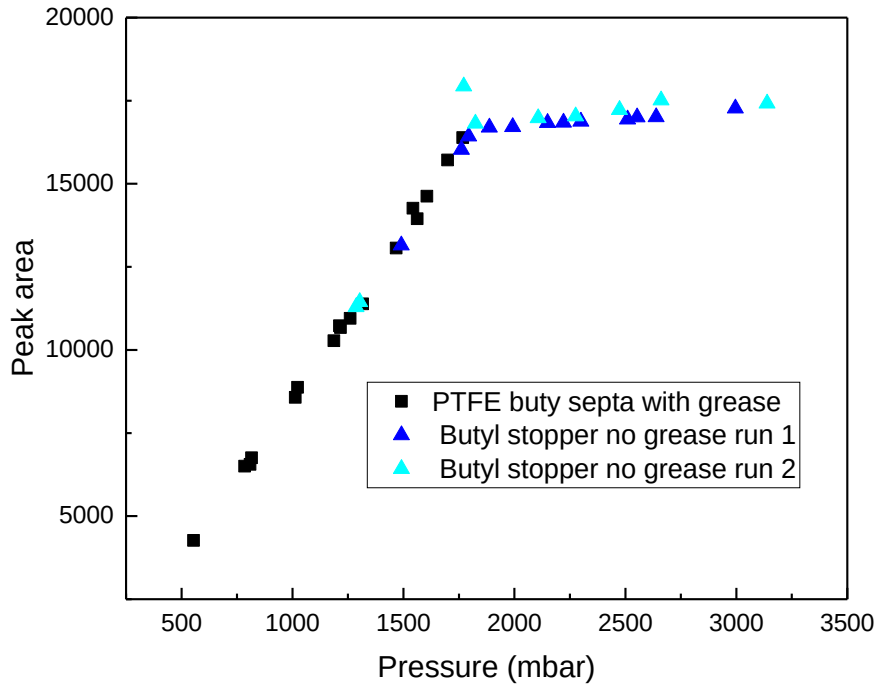

Figure 2 - Calibration curves with CO_2 using two different kinds of septa showing the same trends.

Future work

Initially synthesis of new materials such as macrocycles and novel deep eutectic solvents will take place. These will subsequently be fully characterised via NMR, TGA, DSC and Karl Fisher. After characterisation these materials with then be tested using the described screening method for CO_2 and CH_4 capacity along with CO_2/CH_4 selectivity using mixed gasses.

References

1. F. M. Baena-Moreno, M. Rodríguez-Galán, F. Vega, L. F. Vilches and B. Navarrete, *Int. J. Green Energy*, 2019, **16**, 401–412.
2. M. R. Rodero, R. Ángeles, D. Marín, I. Díaz, A. Colzi, E. Posadas, R. Lebrero and R. Muñoz, in *Biogas*, Springer, 2018, pp. 239–276.
3. J. L. Anthony, J. L. Anderson, E. J. Maginn and J. F. Brennecke, *J. Phys. Chem. B*, 2005, **109**, 6366–6374.
4. P. J. Carvalho and J. A. P. Coutinho, *Energy Environ. Sci.*, 2011, **4**, 4614–4619.